TOPICAL REVIEW — Magnetism, magnetic materials, and interdisciplinary research

# Magnetic nanoparticle-based cancer nanodiagnostics*

Muhammad Zubair Yousaf[a)], Yu Jing(余 靓)[a)], Hou Yang-Long(侯仰龙)[a)†], and Gao Song(高 松)[b)]

[a)] *Department of Materials Science and Engineering, College of Engineering, Peking University, Beijing* 100871, *China*
[b)] *College of Chemistry and Molecular Engineering, Peking University, Beijing* 100871, *China*

(Received 28 March 2013)

Diagnosis facilitates the discovery of an impending disease. A complete and accurate treatment of cancer depends heavily on its early medical diagnosis. Cancer, one of the most fatal diseases world-wide, consistently affects a larger number of patients each year. Magnetism, a physical property arising from the motion of electrical charges, which causes attraction and repulsion between objects and does not involve radiation, has been under intense investigation for several years. Magnetic materials show great promise in the application of image contrast enhancement to accurately image and diagnose cancer. Chelating gadolinium (Gd III) and magnetic nanoparticles (MNPs) have the prospect to pave the way for diagnosis, operative management, and adjuvant therapy of different kinds of cancers. The potential of MNP-based magnetic resonance (MR) contrast agents (CAs) now makes it possible to image portions of a tumor in parts of the body that would be unclear with the conventional magnetic resonance imaging (MRI). Multiple functionalities like variety of targeting ligands and image contrast enhancement have recently been added to the MNPs. Keeping aside the additional complexities in synthetic steps, costs, more convoluted behavior, and effects *in-vivo*, multifunctional MNPs still face great regulatory hurdles before clinical availability for cancer patients. The trade-off between additional functionality and complexity is a subject of ongoing debate. The recent progress regarding the types, design, synthesis, morphology, characterization, modification, and the *in-vivo* and *in-vitro* uses of different MRI contrast agents, including MNPs, to diagnose cancer will be the focus of this review. As our knowledge of MNPs' characteristics and applications expands, their role in the future management of cancer patients will become very important. Current hurdles are also discussed, along with future prospects of MNPs as the savior of cancer victims.

**Keywords:** cancer, magnetic nanoparticle, magnetism, diagnosis, nanotechnology

**PACS:** 87.19.xj, 87.57.–s, 87.61.–c, 87.85.–d **DOI:** 10.1088/1674-1056/22/5/058702

## 1. Introduction

Diagnosis gives insight into a patient's disease. Early medical diagnosis is a key to successful treatment and can save lives. Cancer is among the deadliest diseases around the globe, and its incidence is increasing alarmingly.[1] Regardless of the rapid progress in diagnostic procedures and treatments, the survival rate of cancer victims has shown little progress over the past three decades.[2] There is a need, therefore, to extend novel methodologies and technological advances for the accurate detection of early stages of cancer and for targeted therapies based on cancer-specific markers, which could lead to personalized medicine. Rapid growth in diagnostic nanotechnology has opened new horizons both in clinical care and in the laboratory, suggesting a dramatic future. The published work regarding the application of magnetic nanoparticles (MNPs) purely for *in-vivo* and *in-vitro* cancer diagnoses is limited. So, here in this review, we will discuss how MNPs can be employed to yield diagnostic insights for different cancers. MNPs have been widely used in a variety of molecular or clinical imaging modalities as they are biocompatible, have controllable sizes, and can be easily conjugated to functional groups or ligands in both *in-vivo* and *in-vitro* biological systems. The effectiveness of an imaging technique depends not only on its ability to image quantitatively both morphological and physiological functions of the tissue, but also on the contrast agent used to communicate with biomolecules. Several types of contrast media are used in medical imaging, and they can roughly be categorized based on the imaging modalities where they are used. The use of contrast agents of nanometer scale has become commonplace in medical diagnosis. MNPs have fascinated scientists for over a century and are now heavily utilized in biomedical sciences and engineering as they have long been known to communicate effectively with biomolecules (Fig. 1). Today these materials can be synthesized and modified with various chemical functional groups, which allow them to be conjugated with antibodies, ligands, and drugs of interest, and thus opening a broad range of potential advancements in biotechnology, and more importantly in diagnostic medical imaging via magnetic resonance imaging (MRI) coupled with computed tomography (CT), ultrasound (US), and positron emission tomography (PET). These imag-

*Project supported by the National Natural Science Foundation of China (Grant Nos. 51125001, 51172005, and 90922033), the Research Fellowship for International Young Scientists of the National Natural Science Foundation of China (Grant No. 51250110078), the Doctoral Program of the Education Ministry of China (Grant No. 20120001110078), and the PKU COE-Health Science Center Seed Fund, China.

†Corresponding author. E-mail: hou@pku.edu.cn

 

ing modalities differ not only in resolution, but also in the instrumentation and the type of nanoparticle (NP) that can be employed as its assistant. We try to sum up the huge published literature that portrays unique and non-conventional experimental and physical aspects of various types of MNPs, including the fabrication and design of targeted contrast agents to achieve high quality diagnostic applications. Advances in nanobiotechnology require a profound base and a comprehensive knowledge of biology, engineering techniques, imaging modalities, physics, chemistry, and especially the knowhow of their possible integration in nanoscale. This kind of multidisciplinary association in the research field has enormous prospects for screening, early diagnosis, and most importantly personalized medicine.[3–6]

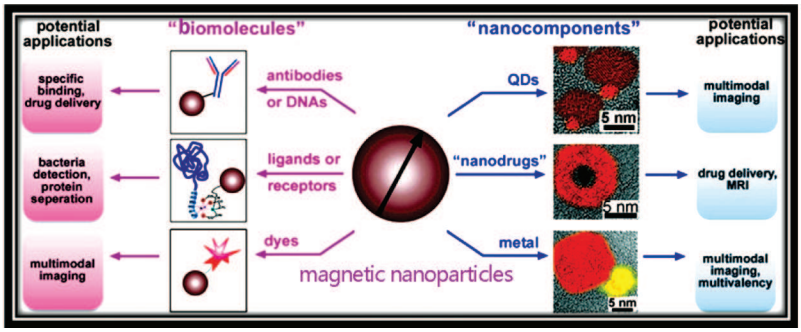


**Fig. 1.** The scheme illustrates two strategies to fabricate multifunctional MNPs and their potential applications.[7]

Practically speaking, the materials synthesized at nanoscale that can attain a high level of response from very small targeted agents are excellent candidates to be used as probes. Up to now, almost all types of nanomaterials have been investigated in various fields of research like bio-sensing, separation, imaging, and therapy, much more than their bulk counterparts. Various parameters like the high volume/surface ratio, surface tailorability, and multi-functionality of nanobiomaterials pose many new promises for biomedicine. Also, the magnetic, intrinsic optical, and/or electrical properties of nanomaterials offer significant prospects in diagnosis when it comes to the complicated and always changing biological settings within the body. Target-specific molecules are now the major players for ultrasensitive detection at the molecular level, and this target-specificity is extremely exploited through the large surface area of nanomaterials, enabling them to attach and bind to a great number of small targets, which in turn make them potentially useful both *in-vitro* and *in-vivo* diagnostics. MNPs are employed in nanotechnology applications to meet the demands of diagnostics for improved sensitivity and speedy detection in complex environmental and biological systems. Finally, we have cited some of the best biomedical and clinical applications of the developed MNPs-based diagnostic architecture, including MRI and diagnostic magnetic resonance (DMR). Toward the end, we describe some ways and means by which this field could be more helpful and practical in the coming years.

## 2. Magnetic resonance imaging

MRI is a noninvasive diagnostic tool that employs magnetic fields to detect the varied water composition in organisms.[8–10] Different water proton relaxivity rates translate into contrasting images of different cells. MRI can be enhanced by reducing the longitudinal and transverse relaxation time of the water protons.[10] It employs the non-ionizing electromagnetic radiation and is considered safe. Excellent cross-sectional images of the internal structures of the body in any plane are produced by radio-frequency (RF) radiation when the body is exposed to carefully controlled magnetic fields. The procedure of image construction in MRI is very simple. A large magnet is applied, which induces a strong external magnetic field causing the nuclei of hydrogen atoms in water to align with the magnetic field. The energy released from the body in response to the RF signal is in turn used by a computer for image construction.[11] It took over 32 years for MRI to become a technique with immense potential for primary diagnostic investigation. MRI is better for cancer screening than magnetic resonance spectroscopy (MRS) and radionuclide techniques, as it can detect cancer at an early stage and with a relatively high spatial resolution. MRI of magnetic nanoparticle-labeled molecular targets has been demonstrated to be able to provide enhanced imaging contrast because the nature and the property of the MNPs can significantly shorten $T_2$ relaxation time (Fig. 2). Several emerging imaging techniques adopt another contrast mechanism, the magnetomotive effect, to actuate embedded MNPs to move periodically inside tissues by applying a controllable external time-varying magnetic field. These tiny mechanical movements can be mea-

sured by a sensitive imaging system to form images. Here are some advantages of MRI: a) It provides detailed images of soft tissues *in-vivo,* unlike other imaging techniques like X-ray, ultrasound, etc. b) MRI contrast agents (CAs) can be directly correlated with local biochemical processes or metabolic activities like blood flow and neuropsychology. c) MRI allows dynamic studies to be performed, like imaging of the beating heart, transport in the vascular system, the movement of joints, and the response of the central nervous system (CNS) to external stimuli.[12] These advantages influence the commercial manufacture of better and improved MRI scanners, where methods for the controlled growth, stabilization, and fictionalization of nanostructures have been imported from the nanotechnology sector to produce a wide range of responsive and smart MRI-detected agents that can be applied to the biomedical field.[13,14]

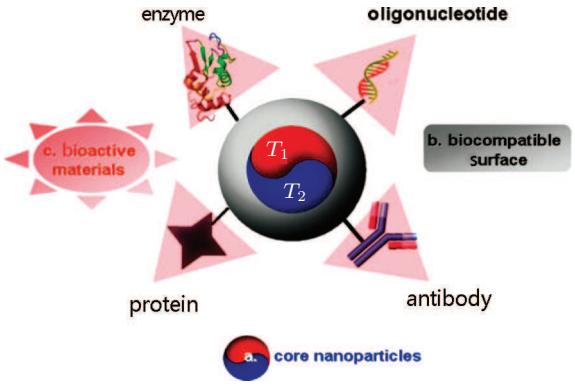


**Fig. 2.** Categories of MRI contrast agents based on NPs.[15]

### 2.1. MRI contrast enhancement using MNPs

Different characteristics of magnetic materials like superparamagnetism, high saturation field, and high field irreversibility enable them to show their potential from nanoscale up to bulk.

With many advantages in diagnostics and biomedicine, the convenient scale of MNPs makes them subject to easy optimization of size and properties. The movement manipulation by an external magnetic force provides tremendous advantages for diagnosis in different locations of the body. MNPs' contrast enhancement ability is based on the signal of magnetic moment of a proton captured by resonant absorption.[7] The unique properties of magnetic nanomaterials to detect tumors, pathogens, proteins, and other active biomolecules have attracted much research interest.[16] Different kinds of MNPs are currently being synthesized by various methods and have previously been reviewed in detail.[17–25]

Contrast agents for MRI are chemical substances that are introduced to the part of the body being imaged. These agents improve the resolution of MRI by increasing or decreasing the brightness between different tissues or between normal and abnormal tissues. Through the use of MRI contrast agents, it is possible to detect smaller tumors, leading to earlier detection of cancer and enhanced treatment, avoiding invasive therapeutic methods. MNPs are excellent candidates for MRI contrast enhancement. Due to their size, they can be easily transported and diffused around the body, and do not require extensive chelating to render them biocompatible, unlike the gadolinium based contrast agents currently used. Also, iron oxide NPs are the only commercial $T_2$ or negative contrast agents, due to their ease of synthesis and biocompatibility. For $T_2$ contrast, healthy tissues/cells take up the NPs while tumor tissues/cells do not. When subjected to MRI, as a result of the presence of iron oxide NPs, the healthy tissue darkens leaving the tumor tissue white, enabling the detection of cancer. However, iron oxides are weakly magnetic, as a result, their contrast enhancement for MRI is limited, and they are limited to detecting superficial tumors just under the skin. The magnetic resonance relaxation time of water in the tissue is altered by the presence of CAs surrounding the tissue, resulting in the increased intensity of water inside the tissue. Gadolinium complexes are used as positive contrast agents or signal enhancement compared to gadolinium chelates such as diethylene triamino pentacetic acid (Gd-DTPA) and MNPs, and are considered more efficient as relaxation enhancers, exhibiting higher relativity and, in particular, a good negative contrast or signal suppression. Their effect on the relaxation measurable at nanomolar concentrations makes nanoparticulate agents in many ways complementary to the gadolinium agents. In addition, the advantages of these nanoagents, such as biocompatibility, selective uptake, targeted delivery, removal from the body, easy adjustment by changing the size and the nature of the surface coating of NPs, are imperative for *in-vivo*

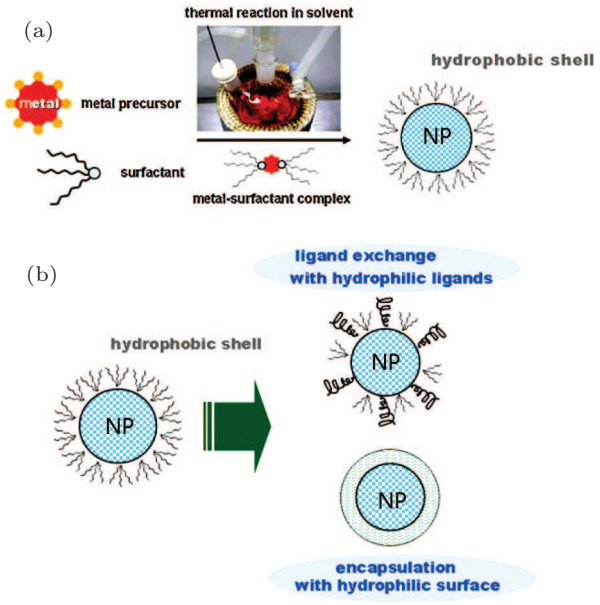


**Fig. 3.** Biocompatible NP synthesis strategy: (a) reaction scheme for monodisperse NPs by thermal reaction under surfactant, (b) surface modification of hydrophobic NPs.[15]

medical applications (see Fig. 3).[12] MNPs can be easily functionalized with molecules, may possess a range of hydrophobic and hydrophilic coatings, which themselves may influence bio-distribution, enabling a wide range of drugs and fluorescent compounds, all of which can be targeted to a specific area or tissue in the body. Proteins or antibodies can be targeted to the surfaces at a molecular, cellular, and/or tissue/tumor level in the body.[26] Moreover, extra potential offered by the magnetic moments can be applied to guide and trap NPs at the target site, where they may be used for a temperature-based response (Fig. 2). Noteworthy efforts have been directed to develop smart contrast agents that would allow the very early detection of various cancers (serving as pre-symptomatic diagnostics) and would potentially be combined with highly effective targeted therapy.[17,23,26,27]

MRI contrast agents are based on different structures. They could be small chelates or may act as macromolecular systems. They could be based on iron oxide NPs. Chemical exchange saturation transfer (CEST) and hyperpolarization agents have previously been discussed along with their magnetic status, composition, bio-distribution, and imaging applications.[28] It is very well known that the expression level of tumor specific molecular markers is very low in normal cells. Specific markers in tumor vessels are particularly well suited for targeted imaging because molecules at the surface of blood vessels are readily accessible to circulating compounds (see Fig. 4).[29]

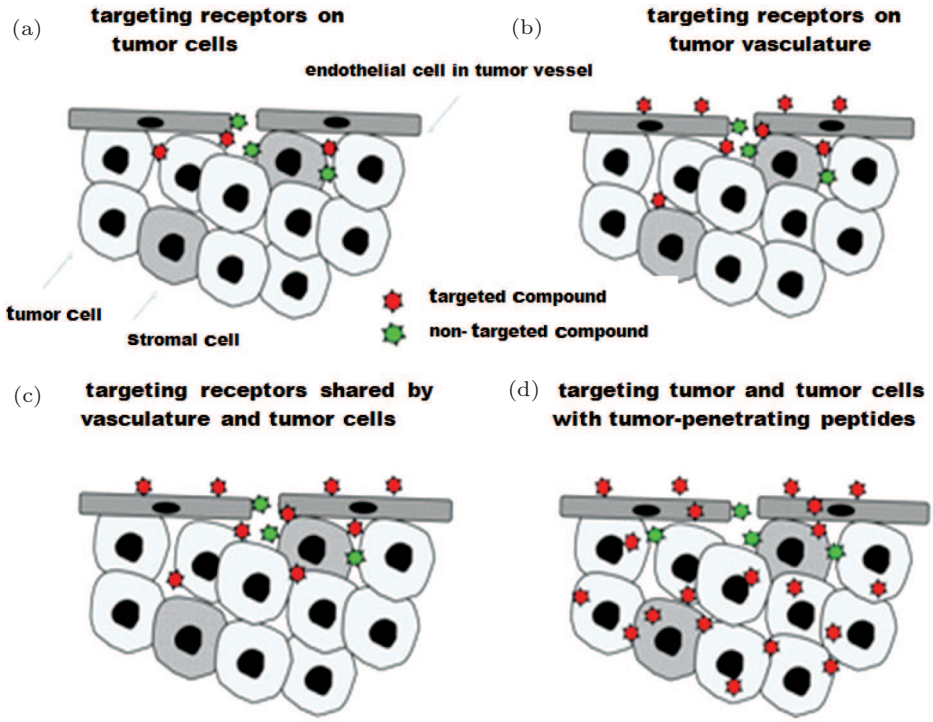


**Fig. 4.** Mechanisms of tumor targeting. (a) Probes that distinguish only tumor cells may accumulate better at a tumor compared to a non-targeted probe. (b) Probes that identify tumor vessels build up in the tumor but do not enter the tumor, using passive mechanisms. (c) Probes that show the combined effectiveness of the two targeting mechanisms to identify both the vessels and tumor cells. (d) Tumor-penetrating targeting probes.[29]

### 2.1.1. Gadolinium (III) based MRI contrast agents

As depicted in Fig. 5, Gd(III) based contrast agents, the first type to be used in MRI, are of different types depending upon the application of enhancements, like extracellular fluidic agents (ionic or neutral), blood pool agents (albumin-binding gadolinium complexes or polymeric gadolinium complexes), and organ specific agents (hepatobiliary), mostly used in the chelated form. The Gd(III) chelates do not pass the blood-brain barrier because they are hydrophilic. Thus, they are useful in contrast-enhancing lesions and tumors where the Gd(III) leaks out. In the rest of the body, Gd(III) initially remains in the circulating blood but is then distributed into interstitial spaces or eliminated by the kidneys.[28] Presently, nine different types of gadolinium-containing contrast agents are available globally.[28] As a free water-soluble ion, gadolinium (III) is somewhat toxic, but is generally regarded as safe when administered as a chelated compound. In animals, the free Gd(III) ion exhibits a 100–200 mg/kg 50% lethal dose (LD50), but the LD50 is increased by a factor of 100 when Gd(III) is chelated, so its toxicity becomes comparable to iodinated X-ray contrast compounds.[30]

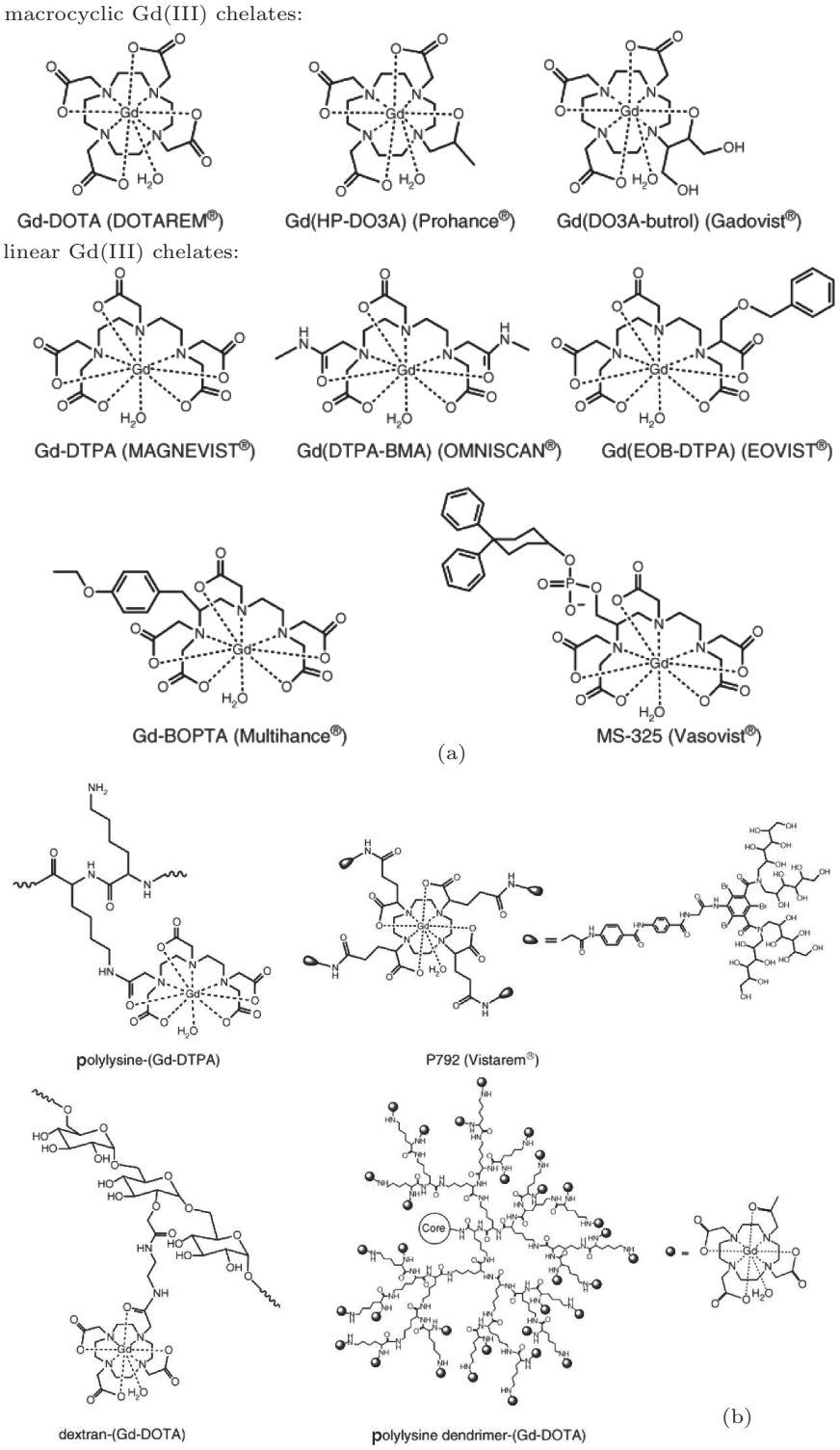


**Fig. 5.** (a) Structures of the Gd(III)-based MRI contrast agents currently used in the clinical practice,[31] (b) examples of macromolecule-based Gd(III) contrast agents.[31]

The chelating carrier molecules for Gd for MRI CA use can be classified by whether they are macro-cyclic or have a linear geometry and whether they are ionic or not. Cyclical ionic Gd(III) compounds are safe as they are considered the least likely to release the Gd(III) ion. However, the use of some Gd(III) chelates in persons with renal diseases is linked to a rare but severe complication, nephrogenic fibrosing dermopathy,[8] also known as nephrogenic systemic fibrosis (NSF). Right now, the NSF has been found to be linked with four gadolinium-containing MRI contrast agents.

The World Health Organization (WHO) issued a restriction on the use of several gadolinium contrast agents in November 2009, stating that there is a high risk in using Gd-containing CAs in liver transplant patients and new-

born babies.[30,32,33] The augmentation is pragmatic when the chelated gadolinium[10] or super paramagnetic iron oxide is used.[9] It is well known that the gadolinium diethylene triamine pentacetate acid (Gd-DTPA)[34] (Tables 1 and 2) has been used more extensively for MRI than any other material. Gd(III) gives contrast and DTPA serves as a chelating ligand forming a complex with Gd(III) to minimize the leaching of the cytotoxic, ionic Gd(III) into the cellular milieu. They can enhance the contrast, but the imaging application of Gd-DTPA is still vulnerable by their rapid renal clearance.[35,36]

**Table 1.** List of Gd(III) based commercially available CAs (adapted from http://www.emrf.org/ and http://www.mr-tip.com/).

| Drug name | Active ingredient(s) | Original approval | Company | Marketing status | Application |
|---|---|---|---|---|---|
| GASTROMARK | FERUMOXSIL | 6-Dec-96 | AMAG PHARMS INC | prescription | gastrointestinal |
| MAGNEVIST | GADOPENTETATE | 2-Jun-88 | BAYER | prescription | lesion |
| | DIMEGLUMINE | | HEALTHCARE | | visualization |
| OMNISCAN | GADODIAMIDE | 8-Jan-93 | GE HEALTHCARE | prescription | neuro/ whole body |
| OPTIMARK | GADOVERSETAMIDE | 8-Dec-99 | MALLINCKRODT | prescription | neuro/ whole body |
| OPTIMARK | GADOVERSETAMIDE | 8-Dec-99 | MALLINCKRODT | prescription | neuro/ whole body |
| IN PLASTIC CONTAINER | | | | | |
| ABLAVAR | GADOFOSVESET | 22-Dec-08 | LANTHEUS | prescription | angiography, |
| | TRISODIUM | | MEDICAL | | capillary permeability |
| EOVIST | GADOXETATE DISODIUM | 03-Jul-08 | BAYER | prescription | liver lesions |
| | | | HEALTHCARE | | |

The second most common benign hepatic tumor is known as focal nodular hyperplasia and can be diagnosed employing liver-specific contrast-enhanced MRI. Multiple and confluent lesions are diagnosed by using gadolinium-dimeglumine as the MRI CA. It is pertinent that focal nodular hyperplasia could be managed successfully and non-invasively, avoiding unnecessary surgery.[37]

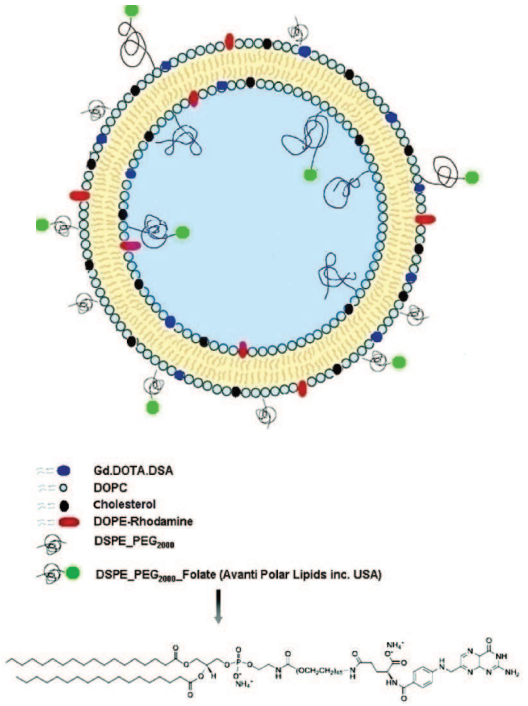


**Fig. 6.** Illustration of folate receptor-targeted bimodal liposomes containing Gd(III) chelates for MR imaging of ovarian cancer.[39]

Extracellular CT and MRI contrast media are found to be reproducible when gadoxetic acid-enhanced MRI is employed. Contrast accumulation in hepatocellular adenomas (HCAs) could be present during the hepatobiliary phase of gadoxetic acid. True hyperintense HCAs during the hepatobiliary phase are rare but in the vast majority of cases are significantly fewer than that in the liver.[38]

The pH of media also plays a role in nanodiagnostics. In acidic media, the Gd-DTPA complex in the nanoprobe's polymeric coating causes a dequenching of the nanoprobe, with a corresponding increase in the $T_1$-weighted MRI signal. An increase in the $1/T_1$ signal in a folate-conjugated nanoprobe (Fig. 6) is observed as a result of its degradation by a HeLa cell's lysosome acidic (pH 5.0) environment in an intracellular release of Gd-DTPA complex with subsequent $T_1$ activation. Also, the co-encapsulation of anti-cancer drug (Taxol) along with the Gd-DTPA within the folate receptor results in the $T_1$ activation of the probe, which in turn concurs with the drug release and the cytotoxic effect *in-vitro*, ensuring that $T_1$ nanoagents show promise for pH based diagnosis of tumors and evaluation of drug targeting by MRI.[40]

Early hepatocellular carcinoma (HCC) and benign hepatocellular nodules are often intermingled, leading to false diagnosis with gadoxetic acid-enhanced MRI (Gd-EOB-MRI). A study of Gd-EOB-MRI was conducted, imaging 34 patients with 29 surgically diagnosed early HCCs and 31 surgically diagnosed benign hepatocellular nodules. Criteria like diffusion-weighted imaging (DWI), the signal intensity at each sequence, the presence of arterial enhancement and washout were noted, led to better diagnostic performance when compared to the conventional imaging criteria (arterial enhance-

ment and wash out). A comparative analysis confirmed that specificity was 100.0% for both criteria, ensuring that diagnostic criteria for Gd-EOB-MRI may help to improve the discrimination of early HCC from benign hepatocellular nodules. MRI findings of $T_1$ hypointensity, $T_1$ hyperintensity, DWI hyperintensity on both low and high $b$-value images ($b = 50$ s·mm$^{-2}$ and 800 s·mm$^{-2}$, respectively), arterial enhancement, late wash out, and hepatobiliary hypo intensity were chosen as the diagnostic criteria. Lesions were supposed to be malignant if they satisfied three or more of the above criteria. The higher sensitivity via Gd-EOB-MRI confirmed its superiority as a diagnostic tool over the conventional method, which is based on the arterial enhancement and washout alone (58.6% vs 13.8%, respectively; $p = 0.0002$).[41]

**Table 2.** Types of Gd(III) based MRI CAs with category, engineered methodology, and the cancer diagnosed.

| Gd(III) based contrast agent type | Sub-category | Engineering methodology | Cancer diagnosed | Reference |
|---|---|---|---|---|
| Macromolecular Gd(III) chelates / complexes based | chelates | Gd-DTPA<br>Gd-DTPA-P846<br>Gd-DTPA-P792 | brain Tumor<br>brain Tumor<br>breast Tumor | [42]<br>[43]<br>[44] |
| | protein based | albumin (Gd-DTPA) | blood and tissue<br>prostate cancer | [45], [46]<br>[47]–[49] |
| | linear polymer based | polylysine<br>dextran | colorectal cancer<br>vascular tissues | [50]–[52]<br>[53], [54] |
| | dendrimer based | PAMAM propylene imine PLL | vasculature liver tumor | [55], [56]<br>[57]–[60]<br>[61], [62] |
| | bio-degradable | polydisulfide | breast tumor | [63]–[66] |
| Liposomal based Gd(III) based | PEG liposome core | encapsulated core surface conjugated encapsulated core dual-mode | solid tumors liver tumor brain tumor glioma brain tumor | [67], [68]<br>[69]<br>[70], [71]<br>[72]<br>[73] |
| Targeted Gd(III) based | | | | |
| | tumor Based | cyclic-RGD CLT1&2 | liver cancer vasculature | [74]<br>[75] |
| | protein based | HER2 EGFR | breast cancer glioma | [76,77]<br>[78] |
| | dendrimer based | antibodies peptides folate | ovarian tumor breast cancer<br>brain tumor<br>epithelial cancer<br>solid tumors<br>ovarian cancer | [79]<br>[80], [81]<br>[81], [82]<br>[83]<br>[84]<br>[85] |
| | liposomal based | antibodies peptides folate | malignant melanoma breast cancer solid tumors | [86]–[88]<br>[39], [62] |

MR and optical imaging based on hyaluronic acid-ceramide (HACE) has also been reported as a conjugating DTPA with HACE for the chelation of gadolinium as an MR contrast agent. The conjugation of Cy5.5 to the HACE shows a homogeneous distribution when particle sizes and shapes are considered during the self-assembly of an HACE-based nanoprobe, found to be non-toxic in both U87-MG (low expression of CD44 receptor) and SCC7 (high expression of CD44 receptor) cells. SCC7 cells' uptake efficiency is better than that of 87-MG cells. An HACE-based nanoprobe is found to be better than a commercial formulation (Magnevist), both *in-vitro* and *in-vivo*. An improved accumulation of the nanoprobe in the tumor region as monitored by an NIRF imaging study ensures that the HACE-based dual-imaging nanoprobe is possibly the best choice to diagnose the cancer, employing passive as well as active tumor targeting.[89]

A tumor's extracellular matrix has an abundance of cancer-related proteins that can be used as biomarkers for cancer molecular imaging. Generation 1 lysine dendrimer interacts with CLT1-dL-(Gd-DOTA)(4) that is blended by conjugating four Gd-DOTA monoamide chelates to produce a CLT1 peptide. The $T$-1 relaxivity of CLT1-dL-(Gd-DOTA)(4) is 40.4 mM$^{-1}\cdot$s$^{-1}$ per molecule (10.1 mM$^{-1}\cdot$s$^{-1}$ per Gd) at 37 °C and 1.5 T. High binding specificity of CLT1 was observed in orthotopic PC3 prostate tumors in mice. Improved tumor contrast enhancement in male athymic nude mice bearing orthotopic PC3 prostate tumor xenografts at a dose of 0.03 mmol Gd/kg confirmed that the peptide-targeted MRI contrast agent has potential for more sensitive MR imaging.[90]

Ultra small paramagnetic $Gd_2O_3$ NPs (mean diameter $< 5$ nm) have the highest Gd density of all paramagnetic contrast agents and can act as contrast agents in MRI, especially

in $T_1$-weighted MRI. High relaxivities and signal enhancement modulated by the interactions of water molecules with $Gd_2O_3$ are due to the optimal surface-to-volume ratio. $Gd_2O_3$ nanocrystals coupled with polyethylene glycol (PEG) by grafting procedures are lengthy and less effective in recovering losses. One-pot synthesized $Gd_2O_3$ coated with PEG, found to be colloidally stable in aqueous media, provides high longitudinal relaxivities and small $r_2/r_1$ ratios ($r_1 = 14.2\ \mathrm{mM}^{-1}\cdot\mathrm{s}^{-1}$ at 60 MHz; $r_2/r_1 = 1.20$) for $T_1$-weighted MRI. F98 glioblastoma multiforme cells labeled with the contrast agent, implanted in mice brains, emerged positively contrasted at least 48 h after implantation, showing the development of the brain tumor in each one of the implanted mice. The comparison of PEG-$Gd_2O_3$ with the commercially available iron oxide NPs shows them as a strong positive contrast enhancement in $T_1$-weighted imaging both *in-vivo* and *in-vitro*.[91]

A retrospective study showed the results of about 1802 imaging studies of MRI of oncology patients performed between March 2009 and July 2012 in the Radiology and Nuclear Medicine Departments of Acıbadem Adana Hospital, Adana, Turkey. On MRI, skeletal muscle metastases mostly revealed an iso-intense signal on $T_1$-weighted images, a heterogeneous high signal with peri-tumoral edema on $T_2$-weighted images, and extensive enhancement with central necrosis on gadolinium-DTPA enhanced images. They concluded that extensive tumoral enhancement, central necrosis, and peri-tumoral edema are highly acceptable features of skeletal muscle metastasis.[92]

Dynamic contrast-enhanced magnetic resonance imaging (DCE-MRI) is mostly employed in accordance with other prognostic factors in rectal cancer diagnosis. Gadolinium contrast-enhanced $T_1$-weighted DCE-MRI with a 3 Tesla scanner of 29 patients with rectal cancer was performed prior to surgery. A time-signal intensity curve with four semi-quantitative parameters (i.e., steepest slope, time to peak, relative enhancement during a rapid rise, and maximal enhancement) and the morphologic prognostic factors (i.e., T stage, N stage, and histologic grade) were noted in addition to tumor angiogenesis. But no significant correlations were found between DCE-MRI parameters and T stage, K-ras mutation, or microsatellite instability that affirms that DCE-MRI is useful in prognostic information regarding angiogenesis and histologic differentiation in rectal cancer.[93]

Gadolinium diffusivity can also quantify the tracer transport in tumors. Fourteen different human xenografts were implanted in 14 mice that were subjected to dynamic contrast-enhanced MRI. Estimations of tracer concentration can be calculated by using a *k*-means clustering algorithm to clearly identify the perfused and necrotic tumor regions exhibiting delayed and slow enhancement.[93]

Chow *et al.*[94] investigated the feasibility of detecting and characterizing liver fibrosis using CLT1 peptide-targeted nanoglobular contrast agent (Gd-P) with dynamic contrast-enhanced magnetic resonance imaging in an experimental mouse model of liver fibrosis at 7 T. Differential enhancements were observed and characterized between the normal and the fibrotic livers using Gd-P at 0.03 mmol/kg, when compared with non-targeted controls (Gd-CP and Gd-C). For Gd-P injection, both the peak and the steady-state $\Delta R_1$ of the normal livers were significantly lower than those after 4 and 8 weeks of $CCl_4$ dosing. Liver fibrogenesis with an increased amount of fibronectin in the extracellular space in insulted livers were confirmed by histological observations. Their results indicated that dynamic contrast-enhanced magnetic resonance imaging with CLT1 peptide-targeted nanoglobular contrast agent can detect and stage liver fibrosis by probing the accumulation of fibronectin in fibrotic livers. The work on gadolinium chelators linked to various substrates to develop MRI contrast agents with high relaxation efficiency spans almost three decades now. Ligand based compounds already used in clinics are approved contrast agents, while new bifunctional chelators, based on complexes, have been reported recently. They show a powerful relaxation effect, quicker complexation kinetics, and simpler synthetic procedures. Some new synthetic strategies have shown great promise recently for bifunctional chelator applications in MRI.[95]

It is reported that about 40% of patients subjected to MRI receive Gd(III)-based CAs. Also the safety and effectiveness for the improved cancer diagnosis is progressing. The relaxivities of Gd(III) chelates can be significantly increased by conjugating biocompatible macromolecules and NPs. The flow of Gd(III) chelates on the NPs and macromolecules after the MRI examinations can be aided by attaching biodegradable structures. Gd(III) CAs that specifically bind to tumor markers can produce significant tumor contrast enhancement at reduced doses, as shown by preclinical studies, and they also demonstrate improved contrast enhancement for MRI as compared to currently available clinical CAs in animal models. Detailed toxicological and pharmaceutical evaluations are still required to determine the safety of the agents and enable further steps in clinical development.[31]

### 2.1.2. Iron oxide NP-based MRI contrast agents

Various NPs have been investigated as MRI contrast agents. Iron oxide NPs have been widely used as MRI contrast agents due to their feature to shorten $T_2^*$ relaxation time in different body parts and organs like spleen, liver, and bone marrow. Currently, superparamagnetic iron oxides (SPIO) and ultra-small SPIO (USPIO) are used extensively

(Table 3). Some of them have been approved by the FDA and commercially available (Abdoscan®, GastroMARK®, Resovist®, Feridex®) while some are in different clinical phases (Supravist®, Combidex®, Clariscan®).[96] SPIOs and USPIOs have even been used for lymph-node imaging, can be functionalized with variety of bio-materials, and facilitate targeted imaging via the site-specific buildup of NPs at specific targets. As far as the preparation of SPIOs and USPIOs is concerned, the reduction and co-precipitation reactions are the conventional methods that employ a mixture of ferrous and/or ferric salts, a hydrophilic polymer in aqueous media, while uniform ferrite NPs with high crystallinity have also been reported, employing the thermal decomposition method of metal precursors using surfactants in organic media. Ligand exchange with water dispersible ligands and encapsulation with biocompatible shells are some of the methods developed to make them water-soluble and biocompatible. Modified uniform ferrite NPs, with improved relaxation properties, have successfully been employed as new $T_2$ MRI contrast agents. Recently, extensive research has been conducted to develop nanoparticle-based $T_1$ contrast agents to overcome the drawbacks of iron oxide nanoparticle-based negative $T_2$ contrast agents.[15]

**Table 3.** List of iron oxide based NPs approved for use as MRI CAs. (Modified from http://www.emrf.org/ and http://www.mr-tip.com/).[114]

| Short name | Generic name[a)] | Trade name | Signal[b)] | Status | Size/nm | Bolus injection | Developer |
|---|---|---|---|---|---|---|---|
| AMI-227 | ferumoxtran-10 (USPIO) | Combidex/sinerem | positive or negative | development | 30 | no | AMAG Pharmaceuticals Inc. (USA) Guerbet, SA (EU) |
| AMI-25 | ferumoxides (SPIO) | Feridex/endorem | negative | for sale | 100 | no | AMAG Pharmaceuticals Inc. (USA) Guerbet, SA (EU) |
| Code 7228 | ferumoxytol (USPIO) | | positive | development | 30 | yes | AMAG Pharmaceuticals Inc. |
| SH U 555 A | ferucarbotran (SPIO) | Resovist/cliavist | negative | for sale (EU, Australia, Japan)/development (USA) | 62 | yes | Bayer Schering Pharma AG |
| SH U 555 C | ferucarbotran (USPIO)4 | Supravist | positive | development | 25 | yes | Bayer Schering Pharma AG |
| NC-100150 | PEG-feron (USPIO) | Clariscan | positive | development (discontinued) | 20 | yes | Amersham Health |

[a)] Short description; [b)] high local concentrations and/or appropriate pulse sequence parameters, negative contrast can be achieved (e.g., first-track bolus).

#### 2.1.2.1. SPIO and ultra small SPIO NPs

SPIO, already approved for clinical use within the human circulatory system, is the main MRI contrast agent for imaging various pathological subjects.[24,97–104] The reduced toxicity and increased biocompatibility of MNPs have been the main aspects of improvement since their use in biomedicine. It is relevant that a lot of work has already been done by different scientists to modify the surface of SPIO NPs in a number of different ways.

SPIO nanoparticles' (SPIONs) signature is easily sensed by MR detection, and the particles are non-toxic and approved for clinical use.[106] They were at first restricted to the neuroaxis. Today, SPIONs are one of the most widely used CAs that can cover all the body regions, providing a better imaging for diagnostic decisions by the physicians. Even so, it is believed that better understanding of its utilization in combination with other techniques or alone to maximize the diagnostic certainty may open still other horizons in the diagnostic world. One of SPION's best capabilities is to shorten $T_2^*$ relaxation time in the liver, spleen, and bone marrow. Ferrite NPs are uniform, and they show high crystallinity and improved $T_2$ MRI contrast relaxation properties. They can also be ornamented with targeting agents, leading to a site-specific build up of NPs at desired pathological locations within the body. The development of NP-based $T_1$ contrast agents to overcome the drawbacks of iron oxide nanoparticle-based negative $T_2$ contrast agents is still being explored.[15] Under this heading we will discuss how MRI contrast enhancement, using different kinds of MNPs and nanostructures, could be more useful than ever.

Nakamura *et al.*[107] compared different contrast agents and found that SPIO-MRI tumor detection results were similar to those found by dynamic CT and plain MRI, but lower than those attained by Gd-based MRI. Different combinations were analyzed with the conclusion that better results were obtained in some combinations than in others. The plain MRI and SPIO-MRI combination should be useful for assessing tumor maturity and for choosing a therapeutic modality, because it is based on blood flow patterns. For the combination of Gd dynamic MRI and SPIO-MRI, the effectiveness varies with intra-tumor blood flow patterns. On the other hand, another study concluded that contrast-enhanced ultrasonography is an important system to forecast the grading pattern of HCC

patients and may be considered as an alternative to SPIO-enhanced MRI.[108]

By PEG coating SPIOs, the $T_2$ relaxivity per particle can be increased by more than 200-fold. *In-vivo* tumor imaging results have demonstrated the potential of SPIOs for clinical applications. Although a quick removal of SPIOs from the circulation may be beneficial for minimizing the background signal generated from unbound SPIOs, longer-circulating SPIOs may increase the chance of binding to the target molecules, thus an enhanced contrast. Adding free coating molecules to an injected SPIO solution can significantly prolong its blood circulation. Additional studies are being conducted on the circulation and bio-distribution of DSPE-PEG coated SPIOs to obtain a better understanding of their pharmacokinetics and the methods to modulate their bioavailability (see Figs. 7 and 8).[105]

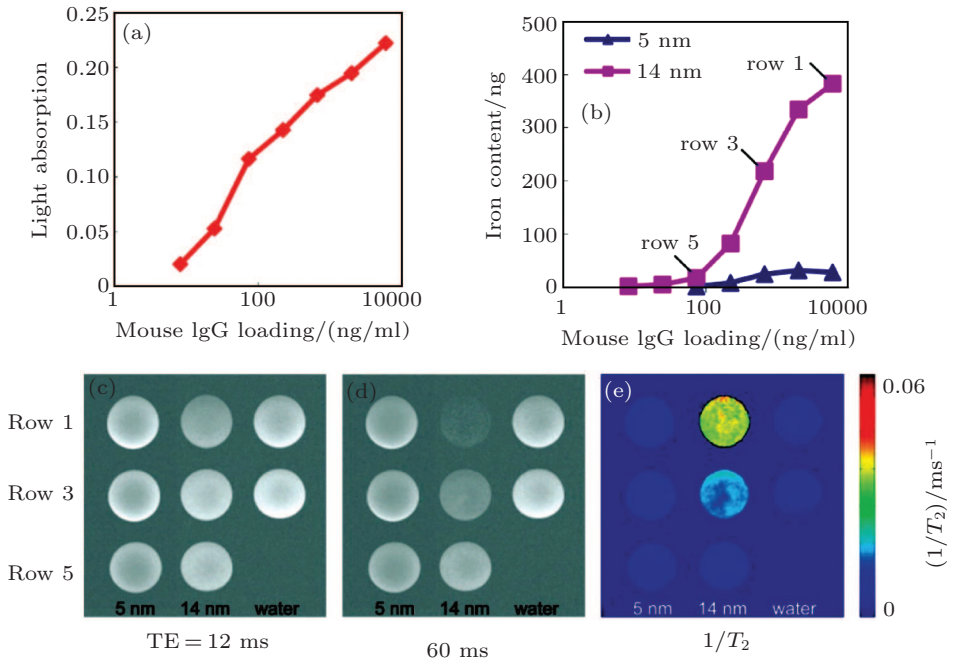


**Fig. 7.** *In-vitro* targeting based on antigens and SPIO: ELISA plates were coated with mouse IgG at selected protein concentrations. The wells coated with mouse IgG were incubated either with antibody conjugated horseradish peroxidase or the SPIOs at 37 °C for 1 h. (a) Wells were incubated with goat anti-mouse IgG conjugated with horseradish peroxidase. Horseradish peroxidase activity was detected by 2,2'-azino-bis(3-ethylbenzothiazoline-6-sulphonic acid) (ABTS). (b) Wells were incubated with SPIOs conjugated with goat anti-mouse IgG. Iron content of bound SPIOs was measured using the ferrozine method. (c) and (d) The plate was loaded with designated amounts of 5 nm or 14 nm SPIOs suspended in 50 μL of water and imaged with a 7 T MRI instrument using spin-echo sequence with echo times of 12 ms and 60 ms, respectively. (e) The $T_2$ effect calculated based on MRI images.[105]

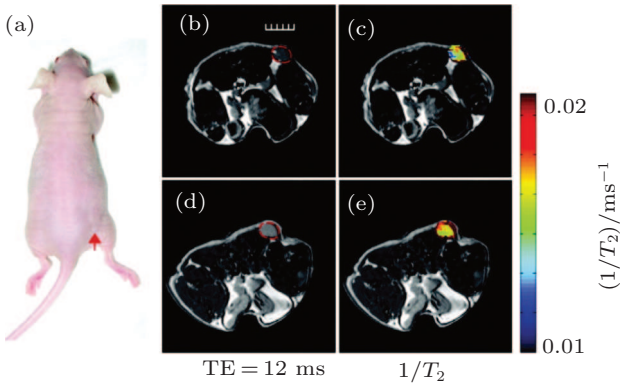


**Fig. 8.** *In-vivo* tumor imaging. MRI experiments were performed using a spin-echo sequence. (a) Arrow shows the location of the subcutaneous tumor. (b) and (c) MR images of tumor before probe injection. (d) and (e) MR images collected after 1 h following the injection of 14 nm SPIONs conjugated with antibodies against mouse VEGFR-1. Red dotted lines in panels (b) and (d) outline the tumor. Scale bar represents 5 mm.[105]

The theoretically predicted maximum of $r_2$ relaxivity is achieved by optimizing the overall size of ferri-magnetic iron oxide NPs. Water-dispersible ferri-magnetic iron oxide nanocubes (WFIONs) with an edge length of 22 nm, encapsulated with PEG-phospholipids, exhibit high colloidal stability in aqueous media. In addition, WFIONs do not affect cell viability at concentrations up to 0.75 mg Fe/ml.

In comparison with the commercialized $T_2$ MRI contrast agents, such as Feridex, the *in-vivo* MR tumor imaging using a clinical 3-T MR scanner with intravenous 22-nm-sized WFIONs injection of enhanced colloidal stability and high $r_2$ relaxivity (761 $\mathrm{mM}^{-1}\cdot\mathrm{s}^{-1}$) is found to exhibit superior $T_2$ contrast effect. The combination of suitable targeting ligands with WFIONs will open the doors to take part indecisive roles in the early diagnosis of tumor metastasis (see Figs. 9–11).[109]

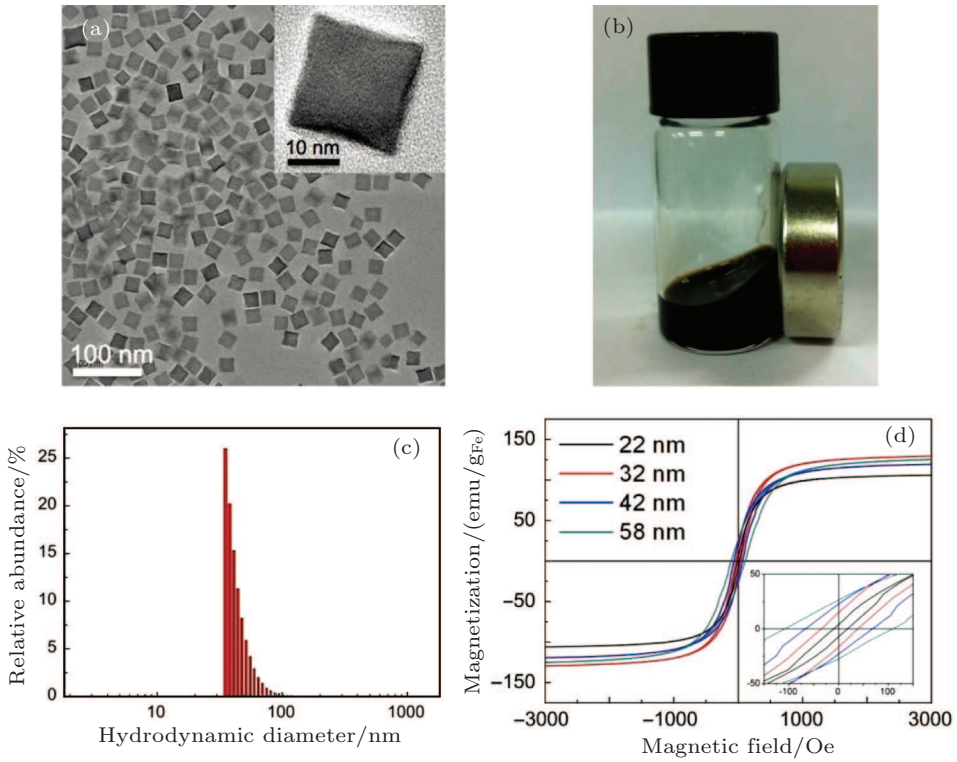


**Fig. 9.** (a) TEM image of 22 nm WFIONs dispersed in water. The average size of WFIONs is $22 \pm 2.6$ nm, and their shape is cubic (inset: HRTEM image). (b) Picture showing high colloidal stability of WFIONs in water. The NPs are not aggregated even in an external magnetic field. (c) DLS data for WFIONs in water. Hydrodynamic diameter of WFIONs is $43 \pm 10$ nm. (d) The *M*–*H* curves of magnetic iron oxide NPs. Whereas the saturation magnetization is independent of the nanoparticle size, the remnant magnetization and coercivity decrease with the decreasing size.[109]

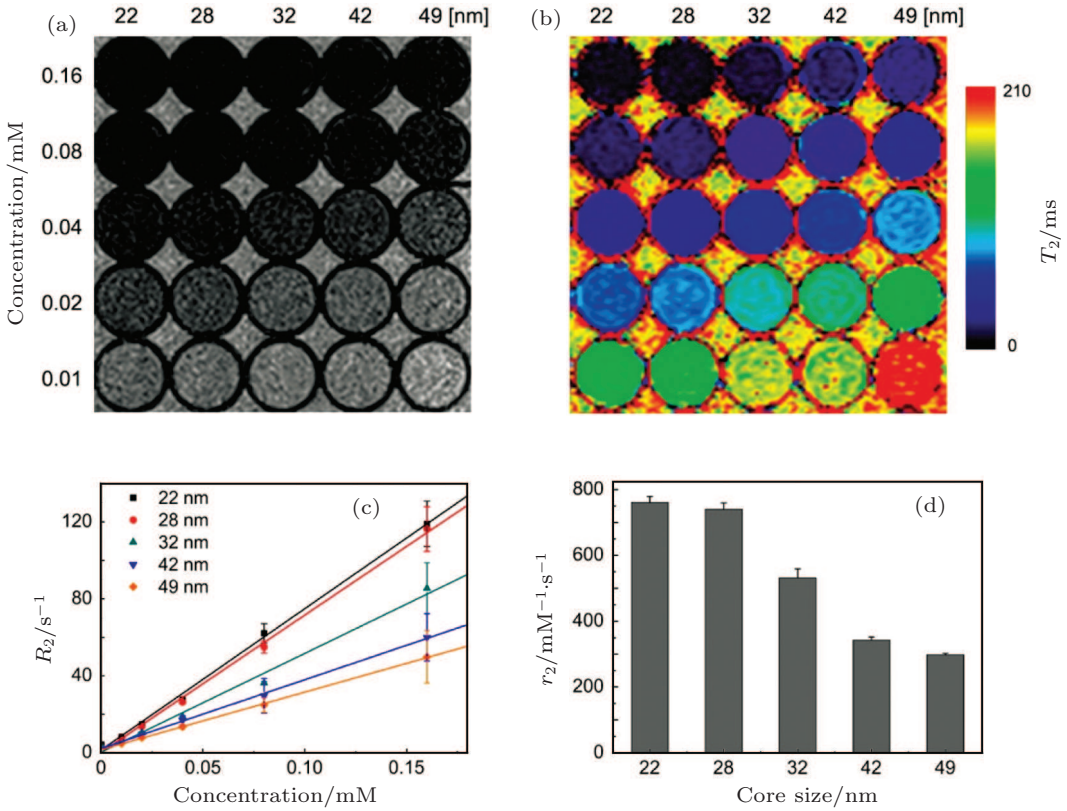


**Fig. 10.** MR contrast effect of ferri-magnetic iron oxide NPs on changes in size. (a) The $T_2$-weighted MR images of ferri-magnetic iron oxide NPs at various concentrations of iron at 3 T, (b) the corresponding color-coded images. (c) Plots of $R_2$ values of ferri-magnetic iron oxide NPs and (d) comparison of their $r_2$ values.[109]

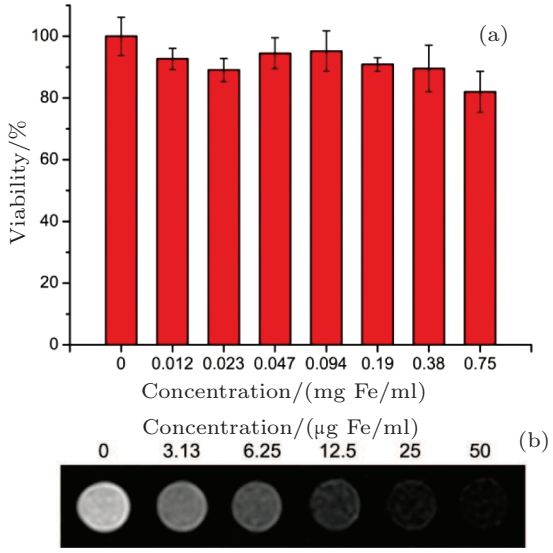


**Fig. 11.** (a) *In-vitro* cytotoxicity test of WFIONs. The viability of the B16F10 cells was determined by an MTT assay after incubation with various concentrations of WFIONs for 24 h ($n$= 3). (b) The $T_2$-weighted MR image of dispersed cells in agarose. The cells were incubated with various concentrations of WFIONs for 24 h.[109]

Two intravenous formulations with nanoscale SPIO particles, ferumoxides and ferucarbotran, are approved specifically for liver MRI. They may be cleared from the blood by phagocytosis, accomplished by a reticuloendothelial system (RES), so that uptake is observed in the normal liver, spleen, bone marrow, and lymph nodes. After the intracellular uptake, SPIOs are metabolized in the lysosomes into a soluble, the non-superparamagnetic form of iron that becomes a part of the normal iron pool (e.g., ferritin, hemoglobin).[110,111]

SPIO-enhanced MRI images are more accurate in the characterization of focal hepatic lesions than the review of SPIO-enhanced images alone.[112] In one study, Feridex®-enhanced $T_2$-weighted images revealed additional lesions not seen on the unenhanced images in 27% of cases and additional lesions not seen by the conventional (non-spiral) CT scans in 40% of cases; the additional information would have changed the therapy in 59% of cases.[113]

The metastasis detection with SPIO CA is also related to the presence or absence of lesions in cancerous cells/tissues and the surrounding cells/tissues. Undifferentiated HCC generally demonstrates no change in signal intensity when compared with $T_2/T_2^*$-weighted images in unenhanced and SPIO-enhanced imaging, resulting in an enhanced contrast-to-noise ratio of the lesion.[115] It is pertinent to mention that some problems in clinical use may arise due to the relative contradiction in the amount of reticuloendothelial cells in focal nodular hyperplasia and hepatic adenoma.

The conjugation of iron oxide NPs and holo-transferrin, and an increased receptor level can affect MRI signals considerably.[115] SPIONs and protein combination may detect apoptotic cells successfully as exhibited both *in-vivo*, in a tumor treated with chemotherapeutic drugs and *in-vitro*, with isolated apoptotic tumor cells and drugs.[116] Recently, monodisperse SPIONs conjugated to amphiphilic copolymers synthesized from methyl methacrylate and PEG methacrylate by atom transfer radical polymerization were conjugated with folic acid. SPION micelles were biologically evaluated by employing MTT in HeLa cells, confirming the potential application of these nanoplatforms for cancer theranostics.[117]

Feridex-labeled cells depicting dual-modality (MR and terahertz (THz) imaging) were assessed using SKOV3 cells at variable concentrations, like 0 mM, 0.35 mM, 0.70 mM, and 1.38 mM. MR and THz images were taken 1 , 3, 7, and 14 days after the inoculation of mice. It was shown that the signal intensities of both THz images and $T_2^*$-weighted MR images of Feridex-labeled SKOV3 increased with increasing Feridex® concentration in a similar pattern, but the signal intensities of *in-vivo* MR and THz images from mice decreased over time. More cellular and molecular studies are needed to further standardize and improve this non-invasive multimodal imaging method as the leading imaging modality.[118] The concept of using USPIONs is not new. Both SPIO and USPIO have shown exceptional hepatic uptake for MRI. However, USPIO preparations may aid in the further characterization of focal liver lesions, as they have displayed greater $T_1$ effect in the liver and in some focal liver lesions.[119] Lots of different methods have been reported for their synthesis, characterization, and potential applications in the diagnosis of different cancers via MRI.[120–124]

### 2.1.3. Mn based MNPs

Paramagnetic chelates and ferro MNPs are developed as MRI contrast agents to effectively improve the tissue contrast by altering the relaxation rates of water protons in the tissue of interest. Although Gd(III)-based CAs are widely used, they are associated with nephrogenic systemic fibrosis (NSF), a disease affecting a small percentage of kidney deficient patients who have a history of exposure to Gd(III)-based contrast agents.[125–127] Due to the problem of NSF, effectual non-gadolinium contrast agents with lesser toxicity may replace Gd(III)-based MRI contrast agents.

An alternative class of MRI contrast agents is paramagnetic manganese (II) chelates or compounds. Manganese-based contrast agents have a distinct bio-distribution pattern and an efficient contrast enhancement in the liver myocardium and brain. An oral formulation of $MnCl_2$ (lumaEnhance) and an intravenous formulation of mangafodipir trisodium (MnDPDP) are commercially available for clinical use.[128,129] An increased dose is desirable to produce enough contrast enhancement, but it may lead to toxicity. Therefore, their relatively low relaxivity is the area of concern that needs to be addressed either by chemical modification or by improving their relaxivities and optimizing their pharmacokinetics and bio-distribution.[59,130–133]

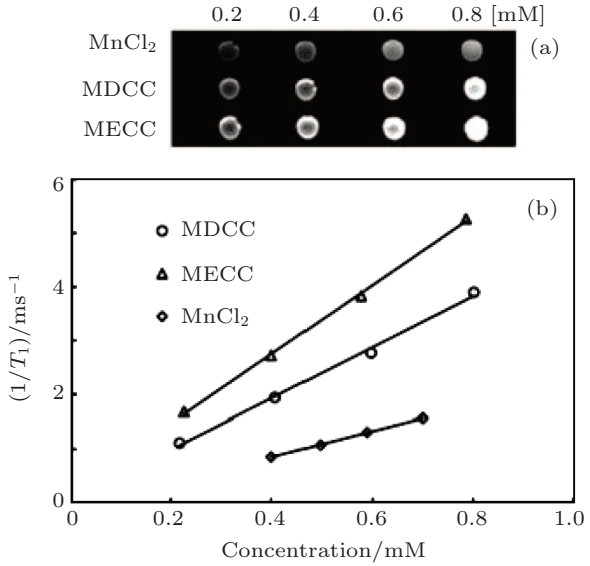


**Fig. 12.** (a) MR images of $MnCl_2$, Mn-DTPA cystamine copolymer (MDCC), and Mn-EDTA cystamine copolymer (MECC) in water as a solvent at the concentrations of 0.2 mM, 0.4 mM, 0.6 mM, and 0.8 mM. (b) The $1/T_1$ versus concentration plot of $MnCl_2$, MDCC, and MECC for the calculation of the longitudinal relaxation rate $R_1$.[134]

Recently, polydisulfide Gd(III) chelates, biodegradable macromolecular MRI contrast agents, were introduced to tackle the safety issue associated with other macromolecular contrast agents. They have prolonged circulation, increased relaxivity, and preferential tumor accumulation as compared to small-molecular Gd(III) chelates.[64,65,135,136] After degradation into oligomeric Gd(III) chelates, they can be excreted via kidneys just after imaging.[137] Manganese (II) and polydisulfides in combination have a better contrast enhancement at a relatively low dose and are very important as far as the safety and toxicity are concerned. After the *in-vivo* contrast enhancement of the agents were evaluated in female nu/nu athymic mice bearing MDA-MB-231 breast cancer xenografts, it was concluded that polydisulfide Mn (II) complexes could serve as non-gadolinium biodegradable macromolecular MRI contrast agents (see Figs. 12–14).[134]

Manganese-enhanced MRI (MEMRI) has been evaluated using human tumor cell proliferation. The relationship between proliferation and calcium influx was explained, and it was found that the MEMRI as a non-invasive method is a better option for investigating this link. The MEMRI is appropriate for the *in-vivo* examination of human prostate cancer.[138]

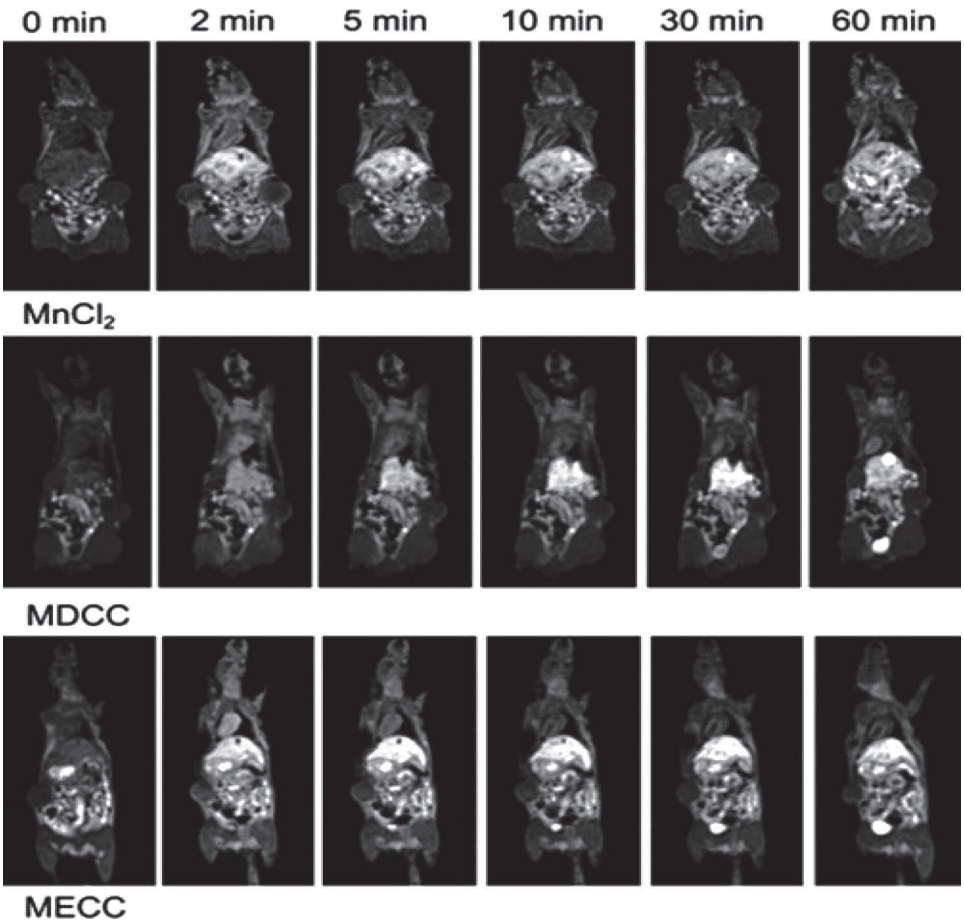


**Fig. 13.** Three dimensional coronal images before (0 min) and at 2 min, 5 min, 10 min, 30 min, and 60 min after the injection of $MnCl_2$, Mn-DTPA cystamine copolymers, and Mn-EDTA cystamine copolymers at a dose of 0.05 mmol Mn(II)/kg.[134]

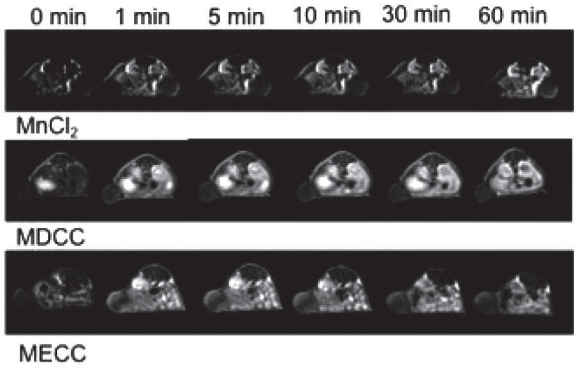


**Fig. 14.** Two dimensional spin-echo images of the tumor before (0 min) and at 2 min, 5 min, 10 min, 30 min, and 60 min after the intravenous injection of $MnCl_2$, Mn-DTPA cystamine copolymers, and Mn-EDTA cystamine copolymers at a dose of 0.05 mmol Mn/kg.[134]

Different combinations of Mn porphyrins-MRI probes, like Mn(III) meso-tetrakis (N-ethylpyridinium-2-yl) porphyrin (MnTE-2-PyP5+) and Mn(III) meso-tetrakis (N-n-hexylpyridinium-2-yl) porphyrin (MnTnHex-2-PyP5+), are used to identify prostate cancer. They imitate powerful superoxide dismutase, peroxy nitrite scavengers and modulators of cellular redox-based signaling pathways through adjunctive anti-neoplastic activity. Phantom studies have shown that they are potentially applicable as novel diagnostic imaging probes as they have 2–3 fold high $T_1$ for both metalloporphyrins in comparison to the commercially available gadolinium chelates. MnTE-2-PyP5+ and MnTnHex-2-PyP5+ have shown MR relaxation changes in prostate tumor xenografts just after a single injection. The capacity of metalloporphyrin for prostate malignancy diagnosis by MRI is proved by the results that show six-fold improvements in contrast enhancements in prostate tumors when compared to surrounding non-cancerous tissues.[139]

Although agglomerates are more efficiently internalized by HT-1080 cells, no clear difference in signal is measured between USP-MnO and SP-MnO-labeled cells at similar concentrations of Mn per cell. Compared with iron oxide particle suspensions in which the agglomeration in aqueous media results in large changes of relaxometric ratios and drastic decreases of signal intensity, the suspensions of MnO particles preserve their MR signal enhancement properties upon agglomeration. These properties could be exploited for more quantitative cell labeling and tracking applications with MRI, using more complex cell cultures such as stem cells, Langerhans islets, or immune cells (See Figs. 15–17).[140]

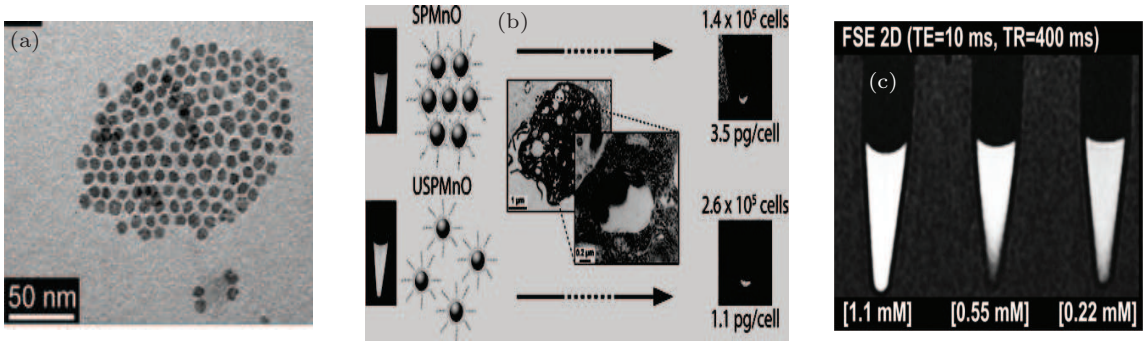


**Fig. 15.** (a) and (b) TEM image and modeling (120 keV) of mono-disperse MnO particles used for relaxometric and cell labeling studies. (c) Dilutions of DMSA-PEG-coated SPMnO, imaged with a $T_1$-weighted MRI spin-echo sequence.[140]

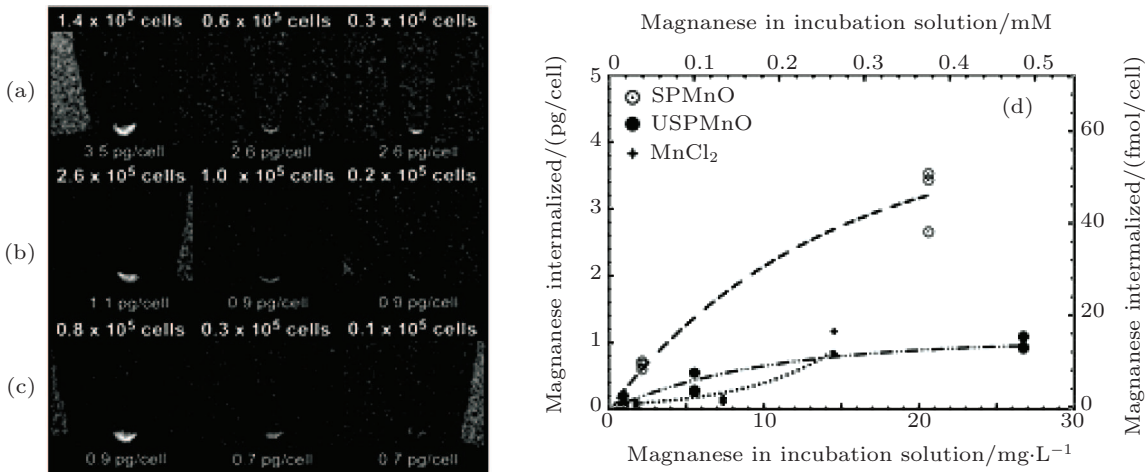


**Fig. 16.** The $T_1$-weighted MR images of HT-1080 cells labeled with (a) SPMnO (0.38 mM), (b) USPMnO (0.49 mM), and (c) $Mn^{2+}$ (0.27 mM). The number under each pellet indicates the mass of Mn detected per cell. (d) Mn uptake in labeled cells, depending on the concentration of Mn in the incubation medium.[140]

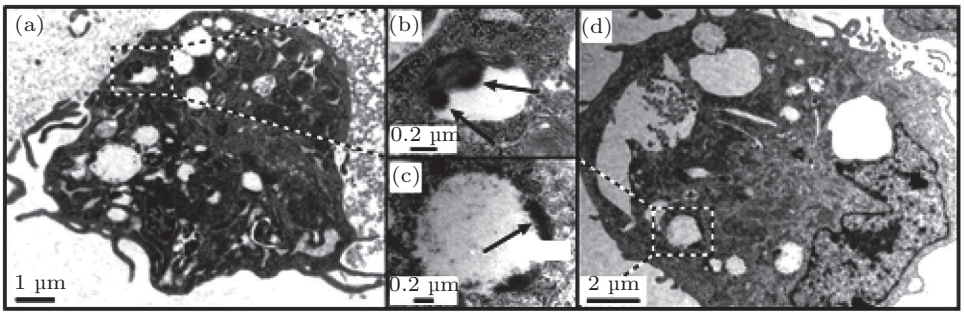


**Fig. 17.** TEM of HT-1080 cells incubated with ((a),(b)) SPMnO and ((c),(d)) USPMnO.[140]

Manganese oxide (MnO) NPs have been proposed as a promising positive MRI contrast agent for cellular and molecular studies. Mn-based contrast agents could enable $T_1$-weighted quantitative cell tracking procedures *in-vivo* based on the signal enhancement.

It is well known that manganese can go into cells via different transport systems, regulated by the plasma membrane calcium sensing receptor (CaSR), so the biological activity of $Mn^{2+}$ ions and their MR contrast agent ability have opened up the possibility of using manganese-enhanced MR imaging (MEMRI) to image functions and pathology of tissues.

### 2.1.4. Magnetic heterostructures

To overcome the disadvantages of Gd-complex based $T_1$ MRI contrast agents, the development of nanoparticulate $T_1$ contrast agents that contain $Gd^{3+}$ or $Mn^{2+}$ ions has been intensively pursued in recent years.[141–143] Gold NPs coated with a monolayer of Gd-complexed, DTPA-based ligand may increase in relaxivity (as compared to small-molecule analogues), presumably due to the limited restriction of rotational diffusion of the nanoparticle-attached Gd ions. The relaxivity can be further increased by self-assembling a polyelectrolyte on the Gd-studded NPs, and NPs can be readily functionalized, as illustrated by co-adsorbing a biotin-based recognition unit.[141] Recent efforts have shown that nanoscale materials, specifically, metal-based NPs, are promising for the expansion of multi-functionalities together and make available the processes and mechanisms to figure out the combination of both drugs and contrast agents in specific organs, tissues, and cells.

Based on the specific sub-cellular locations via DNA hybridization to intracellular targets, Gd(III)-modified DNA-$TiO_2$ semiconducting NP constitutes a novel nanosystem that can target exact DNA sequences. In addition, Gd(III)-modified DNA-$TiO_2$ nanoparticles can also simultaneously be detected via MR imaging in cells (see Figs. 18 and 19).[142]

Bimetallic MR contrast agents like $Au_3Cu_1$ are hollow nanostructures capable of enhanced signal contrast both in $T_1$-weighted and $T_2$-weighted imagings at lower doses. The increased brightness of $T_2$-weighted MR images has resulted in the potential development of this agent for MR angiography.

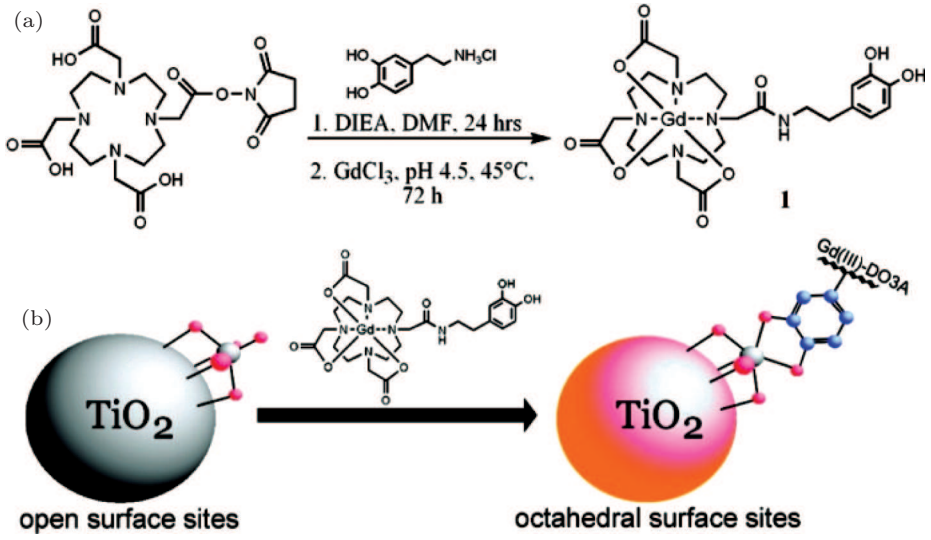


**Fig. 18.** Synthesis programming leading to methodology: (a) dopamine-modified MR contrast agent (DOPA-DO3A), (b) functionalization of $TiO_2$ NPs.[142]

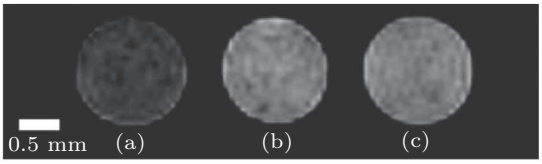


**Fig. 19.** MR images ($T_1$-weighted). The scale bar represents 0.5 mm (at 14.1 T within an FOV of 20 mm and a slice thickness of 0.5 mm). The $T_1$ values are calculated via the student t tests at a 95% confidence level. (a) Control PC3M cells ($T_1 = 3527 \pm 48$ ms); (b) PC3M cells incubated with 0.001 mM DNA-DOPA-DO3A NPs with 1.8% 1:$TiO_2$ active site coverage ($T_1 = 2178 \pm 88$ ms); (c) PC3M cells incubated with 0.001 mM DNA-DOPA-DO3A NPs with 4.4% 1:$TiO_2$ active site coverage ($T_1 = 2356 \pm 100$ ms).[142]

The porous, hollow morphology of the NPs is believed to be linked to the cooperativity originating from the NPs and the large surface area of the water. Amine groups provide an opportunity for the attachment of biological signals on the outermost PEI polymer shell, offering great prospects for multi-modality nanostructures, especially composite capsules. The current study has shown that the conception of a different type of non-Gd- and non-iron oxide-based bimetallic contrast agents is as practical as other contrast agents (see Figs. 20 and 21).[144] Recently, the surface of spherical, nonporous silica NPs ($SiO_2$-NPs) was modified with gadolinium complexes, fluorophores, and cell-penetrating peptides to achieve the multifunctionality of a single particle. The Gd surface concentrations were 9–16 μmol/g, resulting in nanomaterials with high local longitudinal and transversal relaxivities (similar to $1 \times 10^5$ $mm^{-1} \cdot s^{-1} \cdot NP^{-1}$ and $5 \times 10^5$ $mm^{-1} \cdot s^{-1} \cdot NP^{-1}$, respectively). Rapid cellular uptake was observed *in-vitro*; however, larger extracellular agglomerates were also formed. An *in-vivo* administration revealed a fast distribution throughout the body followed by a nearly complete disappearance of fluorescence in all organs except the lungs, liver, and spleen after 24 h. Such NPs have the potential to serve as efficient multimodal probes in molecular imaging.[145]

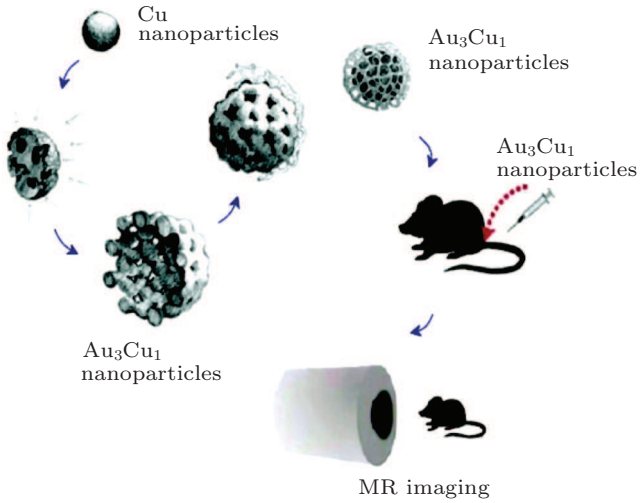


**Fig. 20.** Scheme for $Au_3Cu_1$ nanocapsules used as contrast agents in animal MR imaging.[144]

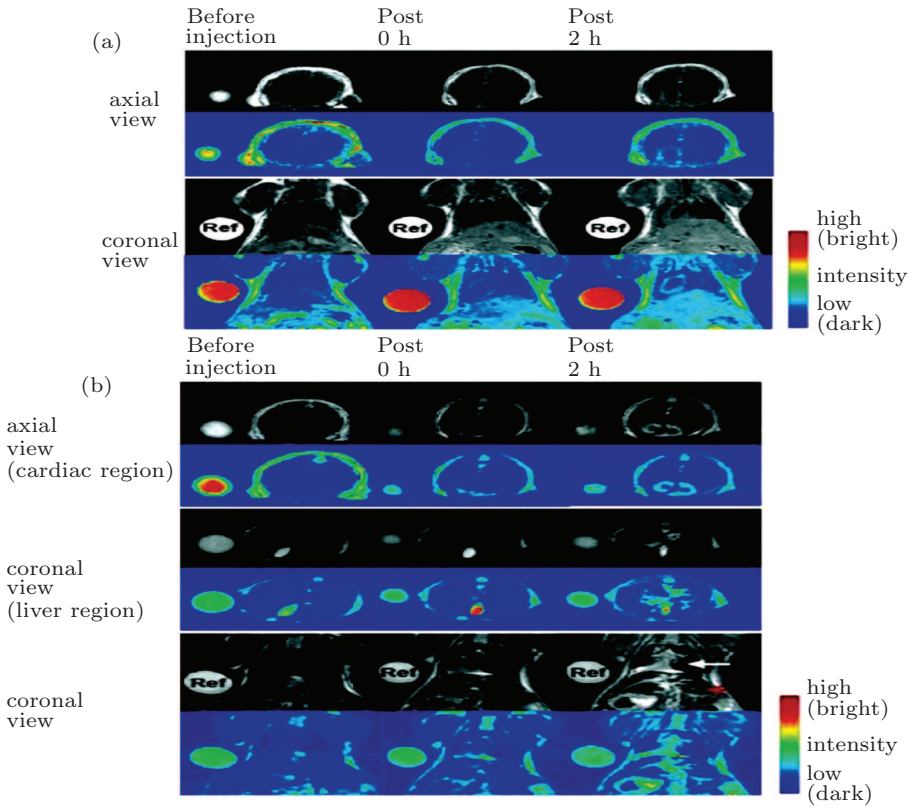


**Fig. 21.** *In-vivo* MRI imaging in male BALB/c mice after injection of $Au_3Cu_1$ nanocapsules: (a) $T_1$-weighted and (b) $T_2$-weighted images at the indicated temporal points (pre-injection, immediately post-injection, and 2 h post-injection). The arrows in panel (b) indicate the increase in signal intensity and show visualized vessels for the thorax and liver regions in $T_2$-weighted images (coronal view).[144]

SPIOs and manganese chloride ($MnCl_2$) are being used for *in-vivo* diagnosis and have shown great promise. The evaluation of therapeutic agents always depends on the efficacy of diagnostic agents for the characterization of early tumor development, especially in MRI. $MnCl_2$ and SPIOs are used to label prostate cancer cells, both *in-vitro* and *in-vivo*, and visualized under 1 T MRI for tracing labeled cells and 7 T MRI for tracking *in-vivo*. The respective tumor volumes and tumor masses are histologically examined. $MnCl_2$ is found to be non-toxic. *In-vivo* $MnCl_2$ labeled cells are detectable from day 4–16, while SPIO labeling allows detection until 4 days after the subcutaneous injection. $MnCl_2$ labeled cells are found to be highly tumorigenic in NOD/SCID mice, and the tumor volume measurement is characterized in a time dependent mode. It is evident that the amount of injected cells is always directly correlated with tumor size and disease progression. In addition, the histological analysis of the induced tumor masses confirms the characteristic morphologies of prostate adenocarcinoma. So, the direct *in-vitro* $MnCl_2$ labeling and 7 T-based *in-vivo* MRI tracing of cancer cells in a model of prostate cancer imply that $MnCl_2$ labeling is suitable for *in-vivo* tracing and may allow long detection stages. High tumorigenic potential, both *in-vivo* and *in-vitro*, makes $MnCl_2$ and SPIOs as ideal candidates for cancer diagnosis. It is noteworthy that this kind of model can also be applied to diagnose other types of cancers.[146]

Measured and confirmed using a vibration magnetometer, non-toxic polymer-based superparamagnetic NPs (P80-TMZ/SPIO-NPs) of 220 nm with a narrow hydrodynamic size distribution serve as a theranostic agent for brain cancer and exhibit high drug loading, encapsulation, and efficient drug release performance for 15 days. Techniques like fluorescence microscopy, Prussian blue staining, and atomic absorption spectrophotometer (AAS) have confirmed their cellular uptake in C6 glioma cells both qualitatively and quantitatively. Also, MRI results have confirmed that Polysorbate 80 coated temozolomide-loaded PLGA-based super paramagnetic NPs are promising as a multi-modal theranostic carrier for brain cancer.[147]

## 3. Diagnostic magnetic resonance

The concept of personalized medicine is appealing, as it provides important modalities like disease diagnosis, malignancy monitoring, and therapy efficacy evaluation in a single shot that in turn depends on the sensitive measurement and quick diagnosis of relevant biomarkers or pathogen/cells in biological samples. When it comes to clinical settings, an assay utilizing the molecular measurement of markers must satisfy some criteria like increased sensitivity and specificity, ease of preparation with a small sample volume, and multiplex based simultaneous recognition of a number of diverse target molecules of interest. We know that the conventional detection strategies based on scattering, absorption, and autofluorescence in optical imaging are often problematic, requiring all-embracing sample purification. The impression of biosensing using MNPs offers exclusive advantages over the conventional diagnosis and screening methodologies and has attained popularity in the recent past because biological samples lack a magnetic background; thus using MNPs can obtain extremely sensitive and specific measurements in spite of the murky and muddy appearance of some biological samples. Presently, the attention in research is focusing on structuring MNPs that would be usable in bio-sensing, especially *in-vitro*. DMR modulates the spin-spin relaxation time of water molecules surrounding molecularly-targeted NPs that serve as proximity sensors to produce specific in-vitro diagnostic data for cancers.

Improvement in DMR detection limits for various target moieties depends on utilizing a broad range of targets like DNA/mRNA, proteins, small molecules/drugs, pathogens like bacteria and viruses, and tumor cells for developing more effective MNP-based biosensors. Miniaturized nuclear magnetic resonance detectors, better MNPs, and novel conjugation methods are examples of the advanced DMR technology. But still there is a dire need to develop DMR based techniques capable of producing accurate results using a minute quantity for a sample. In addition, features like portability, economics, and efficient bio-molecular detection within a biomedical setting are particularly important for the DMR technology to become a highly attractive platform in cancer diagnostics. DMR takes advantage of targeted MNPs to adjust the spin-spin $T_2$ relaxation time of biological samples. Magnetic relaxation switching (MRSw) assay is a kind of DMR that is aimed at small molecular targets with sizes less than or comparable to that of the MNPs. It can detect and quantify the analyte much more precisely and accurately than the conventional methods. The cross linkings of MNPs with metabolites, oligonucleotides, drugs, and proteins support the relaxation switching a lot. MRSw assays can utilize forward switching, a method whereby molecular targets act as cross-linking agents to bring MNPs together into clusters, causing a corresponding decrease in $T_2$; whereas in the reverse switching of MRSw, the enzymatic cleavage or competitive binding of molecular targets disassembles preformed clusters, increasing $T_2$ relaxation. It is noteworthy that MRSw assays are conducted without unbound MNPs being removed.[148]

## 4. Multifunctional MNPs for multimodal probing

Nanostructures provide an excellent platform to integrate different functional nanocomponents into one single nanoentity to exhibit multifunctional properties. Assembling unlike

NPs into a single entity as a novel building block is exciting and holds great potential.

As briefly discussed in the following sections, based on the MNPs, one can combine QDs to exhibit magnetic and fluorescent properties, sequentially grow metallic nanocomponents or form exotic nanostructures, such as yolk-shell NPs for the exploration of nanomedicine.

Intracellular exploitation of MNPs for biological applications offers a practical tool to explore the difference between the apical and basolateral domains in polarized cells by the asymmetric localization of MNPs ornamented with specific ligands. To realize these promises, the fluorescent MNPs should have fast response to a magnetic force, which is yet to be improved.

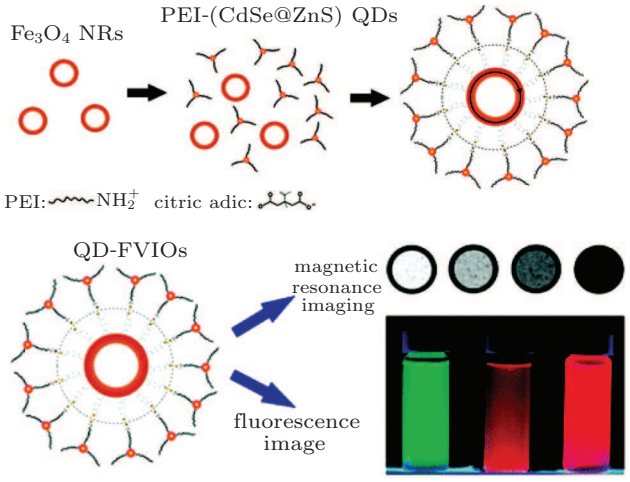


**Fig. 22.** Schematic map for the synthesis of water-dispersible QD-FVIOs. The branched PEI is drawn as simple line for clarity.[149]

A new class of magnetic-fluorescent nanoprobes, QD-FVIOs with elevated luminescence and a magnetic vortex core, have been successfully developed. The biocompatible and multicolor QD-FVIOs have a much stronger effect on $T_2^*$-weighted MRI signals than the conventional SPIO-based multifunctional NPs. Available results from exploratory experiments of multiphoton fluorescence imaging and cell uptake indicate that QD-FVIOs are rapidly internalized by endocytosis and are initially stored in vesicles, followed by slow endosomal escape and release into the cytoplasm. These insights suggest that QD-FVIOs could serve as an excellent dual-modality imaging probe for intracellular imaging and therapeutic applications (see Figs. 22–24).[149]

The features of nanomaterials like high sensitivity, target specificity, stability, and most importantly, biocompatibility are desirable to obtain multifunctional nanoscale diagnostic agents that will facilitate tumor screening and diagnosis after employing the multiplex detection modalities (Figs. 25 and 26).[150,151] For the required functions and specificity to cancer diagnostics, integrated-nanoprobe diagnostic systems could include metals, oxides, polymers, enzymes, and other components in different combinations, versatile structures, and novel compositions.

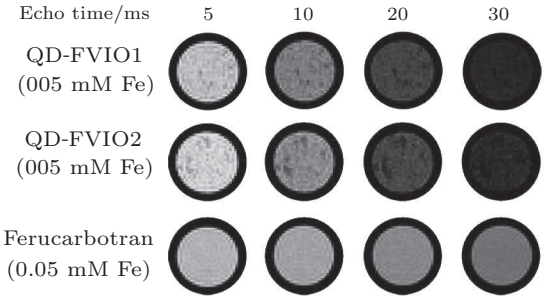


**Fig. 23.** *In-vitro* $T_2^*$ weighted MRI of QD-FVIOs in 2% agarose and commercial ferucarbotran in water.[149]

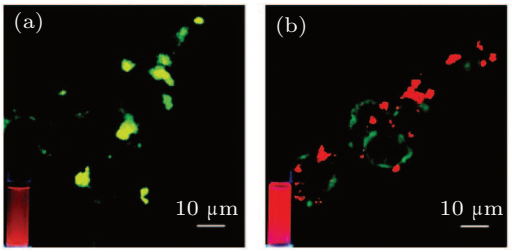


**Fig. 24.** Representative two-photon fluorescence images (756 nm excitation) of the stained MGH bladder cancer cells with (a) yellow- and (b) red-colored internalized QD-FVIOs.[149]

A single nanoparticle probe at molecular level can be used to produce images of cancer and clinically useful measurements both *in-vitro* and *in-vivo*. In the recent past, many studies have been conducted that emphasize the combination of QDs and iron oxide NPs,[152–156] because in cancer diagnostics this combination could give MRI along with fluorescence data, a pairing that is direly needed for multimodal analysis and accurate diagnosis. Concurrent MRI and fluorescence imaging, both *in-vitro* and *in-vivo*, using the hybrid nanostructures containing MNPs and QDs has been reported recently[157] and found to be capable of more accurate and effective early detection of cancer. Another heterodimer comprising $Fe_3O_4$–CdSe NPs has been used very successfully in manipulating and probing NPs within cells,[158] as they straightforwardly deliver the specific ligands to the target moieties on one hand and at the same time enable monitoring of the NP's location inside the cells. To realize the fundamental cellular processes and functions, and to differentiate normal and abnormal cells/tissues, this dual-mode technology can be considered to be a useful tool.

The inherent properties and functions of metallic NPs hold their importance as optical contrast agents and probes. Metallic NPs are mostly used in florescence imaging and also for drug delivery, but the combination of these with MNPs has not been studied extensively, mainly because of some characteristic differences between metals and today's MNPs. But it is likely that in future this combination will prove to be one

of the best. The $Fe_3O_4$–Au heterodimer has been reported as a nanostructure that presents the particles with two distinct surfaces, making it possible to employ different kinds of functional molecules getting attached covalently in addition to their own dissimilar functionalities, $Fe_3O_4$–Au multifunctional heterodimers can bind with specific receptors and respond to external magnetic fields for specific target imaging, and may turn out to exhibit enhanced resonance absorption and dispersion. In breast cancer diagnosis, the dual functionality of EGFRA-conjugated $Fe_3O_4$–Au heterodimer NPs has been verified.[159]

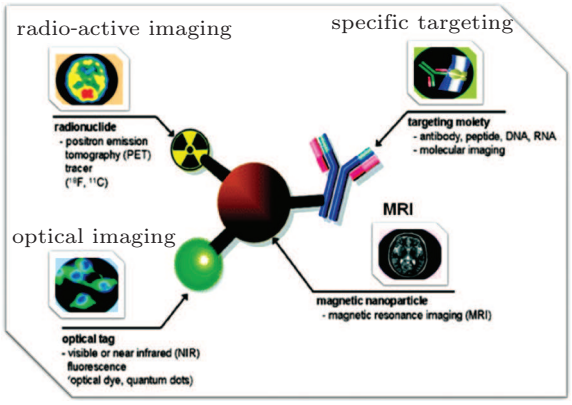


**Fig. 25.** A multi-modality nanoprobe model with its various modalities.[150]

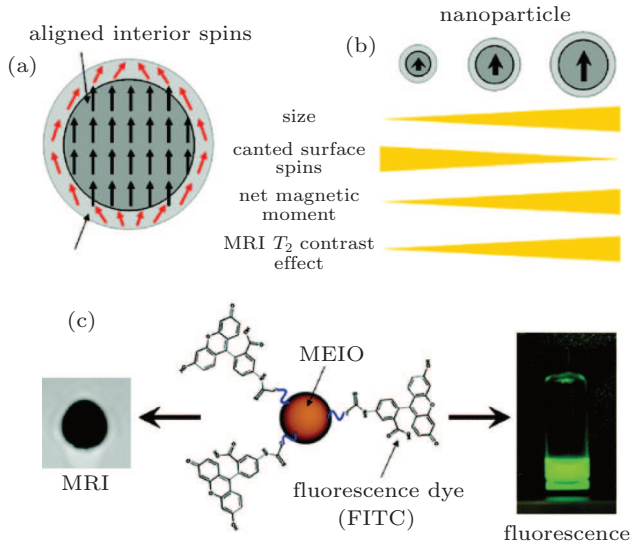


**Fig. 26.** Nanoparticle size effects on magnetism and MR contrast enhancement: (a) canted surface atoms surrounding core magnetic atoms; (b) surface to volume ratio vs size, canted surface spins, net magnetic moment, and $T_2$ contrast effect; (c) MRI-optical dual-mode probes consisting of 12 nm MEIO NPs and FITC fluorescent dye molecules with a dark MRI contrast effect and optical signal.[150]

Scanning confocal microscopy is able to image A431 cells labeled with $Fe_3O_4$–Au heterodimers. In addition, the heterodimer exhibits a strong MR contrast enhancement under an external magnetic field, and thus could be termed as successful nanoscale multi-modal performance of a heterodimer. Various studies have proved that such heterodimers in different combinations show great potential in multiplexed probing and multimodality molecular imaging,[160–162] but some issues, like surface modification, bio-conjugation, and reproducibility, must be resolved before these dimers can realistically be considered for use as a component in *in-vitro* diagnostic applications.

MNPs specifically targeted to the surface of MDA-435 cells *in-vitro* were intravenously administered to rats with glioma. They were internalized, conferring photosensitivity to the cells, and they showed significant MRI contrast enhancement. The pharmacokinetics and distribution of NPs within the tumor were analyzed by serial magnetic resonance imaging. Glioma-bearing rats treated with targeted NPs in combination with photodynamic therapy (PDT) showed a significantly better survival rate than animals that received PDT after the administration of non-targeted NPs. Furthermore, compounds that were found to be excellent photosensitizers but were limited by inherent systemic toxicity could be reevaluated in the context of polymeric nanoparticle encapsulated delivery, as the nanoparticle matrix removes the therapeutic molecule from direct interaction with the physiological milieu (See Fig. 27).[163]

Commercially available SPIOs accumulate in normal lymph tissues after injection at a tumor site, whereas less or no accumulation takes place in metastatic nodes, thus enabling lymphatic staging using MRI. After comparing the findings using histology and vibrating sample magnetometry, the potential of SPIOs like EndoremW (Iron oxide NPs) as novel photoacoustic (PA) contrast agents in biological tissue has been reported using 14 T MR-imaging. The PA setup was able to detect the iron oxide accumulations in all the nodes containing the NPs. The distribution of the PA signal inside the nodes corresponded with both MRI and histological findings. Nodes without SPIO enhancement did not show up in any of the PA scans. EndoremW can be used as a PA contrast agent for lymph node analysis, and a distinction can be made between nodes with the agent and nodes without. This opens up possibilities for intra-operative nodal staging for patients undergoing nodal resections for metastatic malignancies.[164]

By integrating anatomical and molecular based imaging capabilities, multimodal NP based probes are very attractive in the paradigm shift to new imaging technologies, not only at the molecular and cellular levels but also for false-free theranostics that in turn will lead to a better tolerance of fundamental biological developments. Such multimodal probes can be easily extended to therapeutic applications by simply adding drug molecules into the probes or by using the magnetic component as a heat generator for hyperthermia or as a guiding vector to the targeted area. A current flood of attention in nanotechnology has further boosted up the breadth and intensity

of the NP research area. Although still in its early stages with only a handful of successful demonstration cases, the continued development of such multimodal probes is increasingly important for advancing this exciting and rapidly changing research field.[12,150,165–170] Magnetic immunoassay (MIA) is a kind of diagnostic immunoassay exploiting magnetic beads as labels in lieu of the conventional enzymes, radioisotopes, or fluorescent moieties. It engages the specific antibody binding to its antigen, and a magnetic tag is attached to either component of the duo. A magnetometer measures the magnetic field change induced by the beads, leading to the detection of the target molecule. The signal measured by the magnetometer is proportional to the quantity of the analyte (virus, toxin, bacteria, cardiac marker, etc.) in the initial sample.

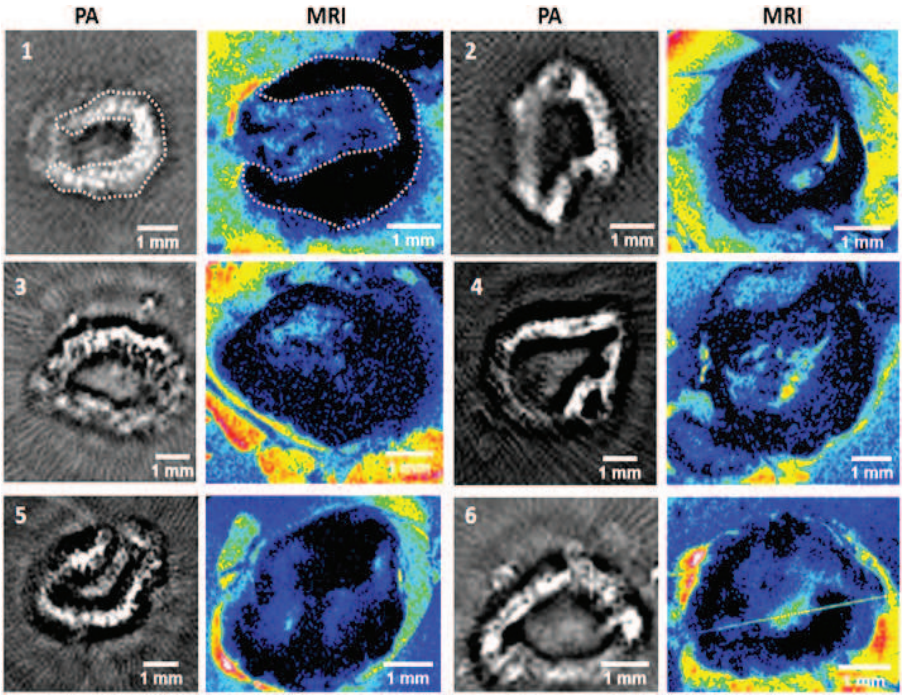


**Fig. 27.** Photoacoustic and MR image comparison of resected lymph nodes with contrast injection. As shown in lymph node 1 (white dotted line), the PA response pattern is comparable with the location of decreased MRI signal. Some nodes show a continuous contrast band throughout their periphery (1,5), while others show some small irregularities (4,6).[164]

## 5. Conclusion and future prospects

Here we have tried to review and summarize recent developments in cancer detection methods with an emphasis on magnetism and nanotechnology. Magnetism has been one of the hottest topics in cancer care and diagnosis in the recent past, and still much is being invested, both in the scientific community and by commercial players. On one hand, nanomaterials have uniquely attractive characteristics for biosensing, while on the other hand various magnetism-based materials and nanotechnology have facilitated precise, specific, and sensitive screening based on cancer biomarkers. Early detection and accurate prognosis of cancers has long been awaited, especially for newly developed cancers that go unchecked because of being asymptomatic. In this respect, the role played by the detection limit is crucial, and nanotechnology can contribute immensely to successfully exploit this property before it is too late. It is not so important to develop new methods for diagnosing cancer after symptoms start appearing, but it is really vital to isolate and detect the smallest presence of cancerous cells, as it maximizes the treatment options and increases the chances of survival, nipping evil in the bud.

Sensing mechanisms are the key to developing such nanoscale high speed vehicles that will push the detection limit down as low as possible. Biomarker discovery is another door that leads to more specific and more sensitive diagnosis and can work precisely with such nanotools. Nanotechnology together with magnetism and biology will undoubtedly help to screen, detect, and diagnose cancer at very early stages, keeping an ever more meticulous eye on the disease. But one has to keep in mind that these new technologies must be evaluated critically before we apply them clinically. Although the idea of capturing cancers at an early stage is very striking and badly needed, the patient safety and environmental quality must still be the top priority, and the journey of nanomaterials through the body and the environment should be fully charted.

Diagnosis is a key factor in the treatment of any disease, including cancer, which is a vile mixture of lots of pathological cells and faulty mechanisms. The early and accurate diagnosis plays a pivotal role in various stages of the ultimate clin-

ical outcome, like treatment options, care and management, severity of disease progression, possible side effects, and the probability of relapse. Here in this review we have tried to address various magnetic materials that can prove to be helpful for the ever important diagnostic paradigms for cancer treatment. There is a whole field of molecular diagnostics that uses things called molecular probes. Again, they go after disease markers. And they have molecules that "light up" when they bind with those disease markers. But it turns out that one can add lots of different functionalities to a nanoparticle to recognize disease markers, to carry a signal to a disease marker, and to amplify the signal at really low NP concentrations. The beauty of nanostructures is that on one hand they are small enough, invisible to the naked eye, and capable of full dispersion in a solution, and on the other they are large enough to be decorated by variety of functional particles. They provide many additive capabilities and variable structures like balls, clusters, stars, cages, dimers, cubes, bricks, webs, shells, flowers, etc. that are not present in the conventional molecular systems. And after the decoration with numerous moieties, they still can be used as a catalyst to generate a lot of signals by associating different functionalities like color, pH, temperature, enzymes concentration, and so on. The chip-based assay has a lot of characteristics associated with it and in the foreseeable future, this chip can operate with just a minimal sample to diagnose cancer by increasing the sensitivity or the magnitude of the signal by flowing ordinary photographic developing solution over the chip. Nanodiagnosis is a whole new and exciting frontier that is likely to have a very big impact on humanity. But the proper learning and precise manufacturing are exceedingly desirable to use these nanostructures safely and to diagnose a variety of cancers and other pathogens. Such technologies are not just dreamed up in ivory towers or a research lab and forgotten. They are technologies that are going to rise and ultimately become available for human use at affordable prices globally. But it takes a long time. These are pretty exciting developments and will end up being used in lots of different types of disease management scenarios including cancer, which is very exciting.

Regarding coating and surface fictionalization of MNPs, a comprehensive approach for new insights to explore monomeric stabilizers, polymeric stabilizers, inorganic coatings, and the vectorization of MNPs for targeted imaging still demands new and novel scientific approaches. Moreover, the properties and characterization of MNP suspensions, like size, morphology, magnetometry, hydrodynamic size, photon correlation spectroscopy, NMR relaxation in the presence of SPIO nanoclusters, improved imaging methods, and improved contrast agents are some of the key areas for future research. Multifunctional masterpieces for multimodal imaging or for imaging cum therapy have been studied extensively, but still most of the published literature regarding NP-based contrast enhancement agents for MRI have not sufficiently addressed some of the most vital issues. It is therefore urged that more studies are undertaken, especially *in-vitro* testing or preliminary animal studies, to make the life-saving technologies commercially accessible. Several key issues like long-term stability, toxicological effects, and pharmacokinetics still have to be addressed before the commercial application of these nanostructures is considered. Multi-disciplinary joint research plans are indispensable to accomplish the crucial ambitions of employing magnetism based MRI contrast agents for active imaging at the cellular and molecular levels that can be functionalized for personalized diagnosis of cancer patients. But after all, we know that despite the evident prospects, the vast majority will be applied only in drug development, basic research, and academics. The pathway to apply them in human care is very lengthy, exhaustive, and costly. Hopefully and optimistically, convergent modeling and straightforward approaches developed by adopting a consistent R&D system may reduce the delay of clinical application.

## References


[1] ten Tije A J, Verweij J, Loos W J and Sparreboom A 2003 *Clin. Pharmacokinet.* **42** 665
[2] Walko C M and Lindley C 2005 *Clin. Ther.* **27** 23
[3] Azzazy H M, Mansour M M and Kazmierczak S C 2006 *Clin. Chem.* **52** 1238
[4] Jain K K 2007 *Clin. Chem.* **53** 2002
[5] Lee W G, Kim Y G, Chung B G, Demirci U and Khademhosseini A 2010 *Adv. Drug. Deliv. Rev.* **62** 449
[6] Tallury P, Malhotra A, Byrne L M and Santra S 2010 *Adv. Drug. Deliv. Rev.* **62** 424
[7] Gao J, Gu H and Xu B 2009 *Accounts Chem. Res.* **42** 1097
[8] Aime S, Castelli D D, Crich S G, Gianolio E and Terreno E 2009 *Accounts Chem. Res.* **42** 822
[9] Aime S, Dastru W, Crich S G, Gianolio E and Mainero V 2002 *Biopolymers* **66** 419
[10] Caravan P, Ellison J J, McMurry T J and Lauffer R B 1999 *Chem. Rev.* **99** 2293
[11] Revett K 2011 *Innovations in Intelligent Image Analysis* (Berlin: Springer-Verlag) p. 127
[12] Pankhurst Q A, Connolly J, Jones S K and Dobson J 2003 *J. Phys. D Appl. Phys.* **36** R167
[13] Gun'ko Y K and Brougham D F 2007 *Nanotechnologies for the Life Sciences* (Baton Rouge: Wiley-VCH) p. 3
[14] Gang H and Bin H 2012 *Appl. Phys. Lett.* **100** 013704
[15] Na H B, Song I C and Hyeon T 2009 *Adv. Mater.* **21** 2133
[16] Perez J M, Josephson L and Weissleder R 2004 *Chem. Bio. Chem.* **5** 261
[17] Corot C, Robert P, Idee J M and Port M 2006 *Adv. Drug. Deliv. Rev.* **58** 1471
[18] Gupta A K and Gupta M 2005 *Biomaterials* **26** 3995
[19] Harisinghani M G, Barentsz J, Hahn P F, Deserno W M, Tabatabaei S, van de Kaa C H, de la Rosette J and Weissleder R 2003 *N. Engl. J. Med.* **348** 2491
[20] Huh Y M, Jun Y W, Song H T, Kim S, Choi J S, Lee J H, Yoon S, Kim K S, Shin J S, Suh J S and Cheon J 2005 *J. Am. Chem. Soc.* **127** 12387
[21] Ito A, Shinkai M, Honda H and Kobayashi T 2005 *J. Biosci. Bioeng.* **100** 1
[22] Lee J H, Huh Y M, Jun Y W, Seo J W, Jang J T, Song H T, Kim S, Cho E J, Yoon H G, Suh J S and Cheon J 2007 *Nat. Med.* **13** 95
[23] Mornet S, Vasseur S, Grasset F and Duguet E 2004 *J. Mater. Chem.* **14** 2161
[24] Neuberger T, Schopf B, Hofmann H, Hofmann M and von Rechenberg B 2005 *J. Magn. Magn. Mater.* **293** 483

[25] Sun C, Lee J S H and Zhang M 2008 *Adv. Drug. Deliv. Rev.* **60** 1252
[26] Gupta A K, Naregalkar R R, Vaidya V D and Gupta M 2007 *Nanomedicine* **2** 23
[27] Laurent S, Forge D, Port M, Roch A, Robic C, Elst L V and Muller R N 2008 *Chem. Rev.* **108** 2064
[28] Geraldes C F G C and Laurent S 2009 *Contrast Media. Mol. Imaging* **4** 1
[29] Ruoslahti E, Bhatia S N and Sailor M J 2010 *J. Cell Biol.* **188** 759
[30] Penfield J G and Reilly R F Jr 2007 *Nat. Clin. Pract. Nephrol.* **3** 654
[31] Zhou Z and Lu Z R 2013 *Wiley Interdiscip. Rev. Nanomed. Nanobiotechnol.* **5** 1
[32] Altun E, Semelka R C and Cakit C 2009 *Acad. Radiol.* **16** 897
[33] Kay J 2008 *Ann. Rheum. Dis.* **67** 66
[34] Sharrna P, Brown S, Walter G, Santra S and Moudgil B 2006 *Adv. Colloid Interface Sci.* **123** 471
[35] Burkhard P 2006 *Nanomed. Nanotechnol. Biol. Med.* **2** 95
[36] Debouttiere P J, Roux S, Vocanson F, Billotey C, Beuf O, Favre-Reguillon A, Lin Y, Pellet-Rostaing S, Lamartine R, Perriat P and Tillement O 2006 *Adv. Funct. Mater.* **16** 2330
[37] Cheng Y C, Chiang C M, Wu C C and Chai J W 2012 *J. Chin. Med. Assoc.* **75** 355
[38] Denecke T, Steffen I G, Agarwal S, Seehofer D, Kroencke T, Haenninen E L, Kramme I B, Neuhaus P, Saini S, Hamm B and Grieser C 2012 *Eur. Radiol.* **22** 1769
[39] Kamaly N, Kalber T, Thanou M, Bell J D and Miller A D 2009 *Bioconjugate Chem.* **20** 648
[40] Santra S, Jativa S D, Kaittanis C, Normand G, Grimm J and Perez J M 2012 *ACS Nano* **6** 7281
[41] Rhee H, Kim M J, Park M S and Kim K A 2012 *Br. J. Radiol.* **85** E837
[42] Fries P, Runge V M, Buecker A, Schuerholz H, Reith W, Robert P, Jackson C, Lanz T and Schneider G 2009 *Invest. Radiol.* **44** 200
[43] Port M, Corot C, Rousseaux O, Raynal I, Devoldere L, Idee J M, Dencausse A, Le Greneur S, Simonot C and Meyer D 2001 *Magn. Reson. Mat. Phys. Biol. Med.* **12** 121
[44] Daldrup H, Shames D M, Wendland M, Okuhata Y, Link T M, Rosenau W, Lu Y and Brasch R C 1998 *Pediatr. Radiol.* **28** 67
[45] Ogan M D, Schmiedl U, Moseley M E, Grodd W, Paajanen H and Brasch R C 1987 *Invest. Radiol.* **22** 665
[46] Schmiedl U, Ogan M, Paajanen H, Marotti M, Crooks L E, Brito A C and Brasch R C 1987 *Radiology* **162** 205
[47] Raatschen H J, Simon G H, Fu Y, Sennino B, Shames D M, Wendland M F, McDonald D M and Brasch R C 2008 *Radiology* **247** 391
[48] Dafni H, Kim S J, Bankson J A, Sankaranaravanapillai M and Ronen S M 2008 *Magn. Reson. Med.* **60** 822
[49] Bhujwalla Z M, Artemov D, Natarajan K, Solaiyappan M, Kollars P and Kristjansen P E G 2003 *Clin. Cancer Res.* **9** 355
[50] Schuhmanngiampieri G, Schmittwillich H, Frenzel T, Press W R and Weinmann H J 1991 *Invest. Radiol.* **26** 969
[51] Curtet C, Maton F, Havet T, Slinkin M, Mishra A, Chatal J F and Muller R N 1998 *Invest. Radiol.* **33** 752
[52] Adam G, Neuerburg J, Spuntrup E, Muhler A, Scherer K and Gunther R W 1994 *J. Magn. Reson. Imaging* **4** 462
[53] Wang S C, Wikstrom M G, White D L, Klaveness J, Holtz E, Rongved P, Moseley M E and Brasch R C 1990 *Radiology* **175** 483
[54] Rebizak R, Schaefer M and Dellacherie E 1998 *Bioconjugate Chem.* **9** 94
[55] Venditto V J, Regino C A S and Brechbiel M W 2005 *Mol. Pharm.* **2** 302
[56] Wiener E C, Brechbiel M W, Brothers H, Magin R L, Gansow O A, Tomalia D A and Lauterbur P C 1994 *Magn. Reson. Med.* **31** 1
[57] Langereis S, de Lussanet Q G, van Genderen M H P, Backes W H and Meijer E W 2004 *Macromolecules* **37** 3084
[58] Langereis S, de Lussanet Q G, van Genderen M H P, Meijer E W, Beets-Tan R G H, Griffioen A W, van Engelshoven J M A and Backes W H 2006 *NMR Biomed.* **19** 133
[59] Kobayashi H and Brechbiel M W 2004 *Curr. Pharm. Biotechnol.* **5** 539
[60] Kobayashi H and Brechbiel M W 2005 *Adv. Drug. Deliv. Rev.* **57** 2271
[61] Luo K, Liu G, She W C, Wang Q Y, Wang G, He B, Ai H, Gong Q Y, Song B and Gu Z W 2011 *Biomaterials* **32** 7951
[62] Storrs R W, Tropper F D, Li H Y, Song C K, Kuniyoshi J K, Sipkins D A, Li K C P and Bednarski M D 1995 *J. Am. Chem. Soc.* **117** 7301
[63] Kaneshiro T L, Ke T, Jeong E K, Parker D L and Lu Z R 2006 *Pharm. Res.* **23** 1285
[64] Lu Z R, Mohs A M, Zong Y and Feng Y 2006 *Int. J. Nanomed.* **1** 31
[65] Lu Z R and Wu X M 2010 *Isr. J. Chem.* **50** 220
[66] Zong Y D, Wang X L, Jeong E K, Parker D L and Lu Z R 2009 *Magn. Reson. Imaging* **27** 503
[67] Mayer L D, Masin D, Nayar R, Boman N L and Bally M B 1995 *Br. J. Cancer* **71** 482
[68] Papahadjopoulos D, Allen T M, Gabizon A, Mayhew E, Matthay K, Huang S K, Lee K D, Woodle M C, Lasic D D, Redemann C and Martin F J 1991 *Proc. Natl. Acad. Sci. USA* **88** 11460
[69] Unger E C, Macdougall P, Cullis P and Tilcock C 1989 *Magn. Reson. Imaging* **7** 417
[70] Krauze M T, Forsayeth J, Park J W and Bankiewicz K S 2006 *Pharm. Res.* **23** 2493
[71] Mamot C, Nguyen J B, Pourdehnad M, Hadaczek P, Saito R, Bringas J R, Drummond D C, Hong K L, Kirpotin D B, McKnight T, Berger M S, Park J W and Bankiewicz K S 2004 *J. Neuro-Oncol.* **68** 1
[72] Karathanasis E, Park J, Agarwal A, Patel V, Zhao F, Annapragada A V, Hu X and Bellamkonda R V 2008 *Nanotechnology* **19** 315101
[73] Ghaghada K B, Ravoori M, Sabapathy D, Bankson J, Kundra V and Annapragada A 2009 *Plos One* **4** e7628
[74] Park J A, Lee J J, Jung J C, Yu D Y, Oh C, Ha S, Kim T J and Chang Y M 2008 *Chem. Bio. Chem.* **9** 2811
[75] Pilch J, Brown D M, Komatsu M, Jarvinen T A H, Yang M, Peters D, Hoffman R M and Ruoslahti E 2006 *Proc. Natl. Acad. Sci. USA* **103** 2800
[76] Artemov D 2003 *J. Cell. Biochem.* **90** 518
[77] Artemov D, Mori N, Ravi R and Bhujwalla Z M 2003 *Cancer Res.* **63** 2723
[78] Shazeeb M S, Sotak C H, DeLeo M and Bogdanov A 2011 *Cancer Res.* **71** 2230
[79] Xu H, Regino C A S, Koyama Y, Hama Y, Gunn A J, Bernardo M, Kobayashi H, Choyke P L and Brechbiel M W 2007 *Bioconjugate Chem.* **18** 1474
[80] Zhu W L, Mollie B, Bhujwalla Z M and Artemov D 2008 *Magn. Reson. Med.* **59** 679
[81] Huang R Q, Han L, Li J F, Liu S H, Shao K, Kuang Y Y, Hu X, Wang X X, Lei H and Jiang C 2011 *Biomaterials* **32** 5177
[82] Han L A, Li J F, Huang S X, Huang R Q, Liu S H, Hu X, Yi P W, Shan D, Wang X X, Lei H and Jiang C 2011 *Biomaterials* **32** 2989
[83] Swanson S D, Kukowska-Latallo J F, Patri A K, Chen C Y, Ge S, Cao Z Y, Kotlyar A, East A T and Baker J R 2008 *Int. J. Nanomed.* **3** 201
[84] Reddy J A, Xu L C, Parker N, Vetzel M and Leamon C P 2004 *J. Nucl. Med.* **45** 857
[85] Parker N, Turk M J, Westrick E, Lewis J D, Low P S and Leamon C P 2005 *Anal. Biochem.* **338** 284
[86] Sipkins D A, Cheresh D A, Kazemi M R, Nevin L M, Bednarski M D and Li K C P 1998 *Nat. Med.* **4** 623
[87] Vaccaro M, Accardo A, D'Errico G, Schillen K, Radulescu A, Tesauro D, Morelli G and Paduano L 2007 *Biophys. J.* **93** 1736
[88] Accardo A, Tesauro D, Roscigno P, Gianolio E, Paduano L, D'Errico G, Pedone C and Morelli G 2004 *J. Am. Chem. Soc.* **126** 3097
[89] Cho H J, Yoon H Y, Koo H, Ko S H, Shim J S, Cho J H, Park J H, Kim K, Kwon I C and Kim D D 2012 *J. Control. Release* **162** 111
[90] Wu X M, Burden-Gulley S M, Yu G P, Tan M Q, Lindner D, Brady-Kalnay S M and Lu Z R 2012 *Bioconjugate Chem.* **23** 1548
[91] Faucher L, Tremblay M, Lagueux J, Gossuin Y and Fortin M A 2012 *ACS Appl. Mater. Interfaces* **4** 4506
[92] Arpaci T, Ugurluer G, Akbas T, Arpaci R B and Serin M 2012 *Eur. Rev. Med. Pharmacol. Sci.* **16** 2057
[93] Koh T S, Hartono S, Thng C H, Lim T K H, Martarello L and Ng Q S 2013 *Magn. Reson. Med.* **69** 269
[94] Chow A M, Tan M, Gao D S, Fan S J, Cheung J S, Qiao Z, Man K, Lu Z R and Wu E X 2013 *Invest. Radiol.* **48** 46
[95] Frullano L and Caravan P 2011 *Curr. Org. Synth.* **8** 535
[96] Qiao R, Yang C and Gao M 2009 *J. Mater. Chem.* **19** 6274
[97] Cengelli F, Maysinger D, Tschudi-Monnet F, Montet X, Corot C, Petri-Fink A, Hofmann H and Juillerat-Jeanneret L 2006 *J. Pharmacol. Exp. Ther.* **318** 108
[98] Kim D K, Mikhaylova M, Wang F H, Kehr J, Bjelke B, Zhang Y, Tsakalakos T and Muhammed M 2003 *Chem. Mat.* **15** 4343
[99] Lee H, Lee E, Kim D K, Jang N K, Jeong Y Y and Jon S 2006 *J. Am. Chem. Soc.* **128** 7383

[100] Leuschner C, Kumar C S S R, Hansel W, Soboyejo W, Zhou J and Hormes J 2006 *Breast Cancer Res. Treat.* **99** 163
[101] Ma H l, Qi X T, Maitani Y and Nagai T 2007 *Int. J. Pharm.* **333** 177
[102] Mahmoudi M, Simchi A and Imani M 2009 *J. Phys. Chem. C* **113** 9573
[103] Pawelczyk E, Arbab A S, Chaudhry A, Balakumaran A, Robey P G and Frank J A 2008 *Stem Cells.* **26** 1366
[104] Talelli M, Rijcken C J F, Lammers T, Seevinck P R, Storm G, van Nostrum C F and Hennink W E 2009 *Langmuir* **25** 2060
[105] Tong S, Hou S, Zheng Z, Zhou J and Bao G 2010 *Nano Lett.* **10** 4607
[106] Nunn A V W, Barnard M L, Bhakoo K, Murray J, Chilvers E J and Bell J D 1996 *FEBS Lett.* **392** 295
[107] Nakamura H, Ito N, Kotake F, Mizokami Y and Matsuoka T 2000 *J. Gastroenterol.* **35** 849
[108] Inoue T, Kudo M, Watai R, Pei Z, Kawasaki T, Minami Y, Chung H, Fukunaga T, Awai K and Maenishi O 2005 *J. Gastroenterol.* **40** 1139
[109] Lee N, Choi Y, Lee Y, Park M, Moon W K, Choi S H and Hyeon T 2012 *Nano Lett.* **12** 3127
[110] Bonnemain B 1998 *J. Drug Target.* **6** 167
[111] Wang Y X J, Hussain S M and Krestin G P 2001 *Eur. Radiol.* **11** 2319
[112] Reimer P, Jahnke N, Fiebich M, Schima W, Deckers F, Marx C, Holzknecht N and Saini S 2000 *Radiology* **217** 152
[113] Ros P R, Freeny P C, Harms S E, Seltzer S E, Davis P L, Chan T W, Stillman A E, Muroff L R, Runge V M, Nissenbaum M A and Jacobs P M 1995 *Radiology* **196** 481
[114] Neuwelt E A, Hamilton B E, Varallyay C G, Rooney W R, Edelman R D, Jacobs P M and Watnick S G 2009 *Kidney Int.* **75** 465
[115] Ba-Ssalamah A, Uffmann M, Saini S, Bastati N, Herold C and Schima W 2009 *Eur. Radiol.* **19** 342
[116] Blankenberg F G, Katsikis P D, Storrs R W, Beaulieu C, Spielman D, Chen J Y, Naumovski L and Tait J F 1997 *Blood* **89** 3778
[117] Mahajan S, Koul V, Choudhary V, Shishodia G and Bharti A C 2013 *Nanotechnology* **24**
[118] Jae Yeon P, Hyuck Jae C, Gi-Eun N, Kyoung-Sik C and Joo-Hiuk S 2012 *IEEE Trans. Tera. Sci. Technol.* **2** 93
[119] Mergo P J, Engelken J D, Helmberger T and Ros P R 1998 *J. Magn. Reson. Imaging* **8** 1073
[120] Bumb A, Brechbiel M W, Choyke P L, Fugger L, Eggeman A, Prabhakaran D, Hutchinson J and Dobson P J 2008 *Nanotechnology* **19**
[121] Jiang T, Zhang C, Zheng X, Xu X, Xie X, Liu H and Liu S 2009 *Int. J. Nanomed.* **4** 241
[122] Li M, Kim H S, Tian L, Yu M K, Jon S and Moon W K 2012 *Theranostics* **2** 76
[123] Tetsumura A, Nakamura S, Yoshino N, Watanabe H, Kuribayashi A, Nagumo K, Okada N, Sasaki T and Kurabayashi T 2012 *Dentomaxillofac. Radiol.* **41** 55
[124] Yang H M, Lee H J, Jang K S, Park C W, Yang H W, Do Heo W and Kim J D 2009 *J. Mater. Chem.* **19** 4566
[125] Aime S and Caravan P 2009 *J. Magn. Reson. Imaging* **30** 1259
[126] Kribben A, Witzke O, Hillen U, Barkhausen J, Daul A E and Erbel R 2009 *J. Am. Coll. Cardiol.* **53** 1621
[127] Kuo P H 2008 *J. Am. Coll. Radiol.* **5** 29
[128] Lee J H and Koretsky A P 2004 *Curr. Pharm. Biotechnol.* **5** 529
[129] Silva A C, Lee J H, Aoki L and Koretsky A R 2004 *NMR Biomed.* **17** 532
[130] Bertin A, Steibel J, Michou-Gallani A I, Gallani J L and Felder-Flesch D 2009 *Bioconjugate Chem.* **20** 760
[131] Pan D, Caruthers S D, Hu G, Senpan A, Scott M J, Gaffney P J, Wickline S A and Lanza G M 2008 *J. Am. Chem. Soc.* **130** 9186
[132] Pan D P J, Senpan A, Caruthers S D, Williams T A, Scott M J, Gaffney P J, Wickline S A and Lanza G M 2009 *Chem. Commun.* 3234
[133] Tan M Q, Ye Z, Jeong E K, Wu X M, Parker D L and Lu Z R 2011 *Bioconjugate Chem.* **22** 931
[134] Zhen Y, Eun-Kee J, Xueming W, Mingqian T, Shouyu Y and Zheng-Rong L 2012 *J. Magn. Reson. Imaging* **35** 737
[135] Lu Z R, Parker D L, Goodrich K C, Wang X H, Dalle J G and Buswell H R 2004 *Magn. Reson. Med.* **51** 27
[136] Zong Y, Guo J, Ke T, Mohs A M, Parker D L and Lu Z R 2006 *J. Control. Release.* **112** 350
[137] Feng Y, Zong Y D, Ke T Y, Jeong E K, Parker D L and Lu Z R 2006 *Pharm. Res.* **23** 1736
[138] Braun R D, Bissig D, North R, Vistisen K S and Berkowitz B A 2012 *Plos One* **7**
[139] Mouraviev V, Venkatraman T N, Tovmasyan A, Kimura M, Tsivian M, Mouravieva V, Polascik T J, Wang H, Amrhein T J, Batinic-Haberle I and Lascola C 2012 *J. Endourol.* **26** 1420
[140] Létourneau M, Tremblay M, Faucher L, Rojas D, Chevallier P, Gossuin Y, Lagueux J and Fortin M A 2012 *J. Phys. Chem. B* **116** 13228
[141] Warsi M F, Adams R W, Duckett S B and Chechik V 2010 *Chem. Commun.* **46** 451
[142] Endres P J, Paunesku T, Vogt S, Meade T J and Woloschak G E 2007 *J. Am. Chem. Soc.* **129** 15760
[143] Na H B, Lee J H, An K, Park Y I, Park M, Lee I S, Nam D H, Kim S T, Kim S H, Kim S W, Lim K H, Kim K S, Kim S O and Hyeon T 2007 *Angew. Chem. Int. Ed.* **46** 5397
[144] Su C H, Sheu H S, Lin C Y, Huang C C, Lo Y W, Pu Y C, Weng J C, Shieh D B, Chen J H and Yeh C S 2007 *J. Am. Chem. Soc.* **129** 2139
[145] Joshi R, Feldmann V, Koestner W, Detje C, Gottschalk S, Mayer H A, Sauer M G and Engelmann J 2013 *Biol. Chem.* **394** 125
[146] Sterenczak K A, Meier M, Glage S, Meyer M, Willenbrock S, Wefstaedt P, Dorsch M, Bullerdiek J, Escobar H M, Hedrich H and Nolte I 2012 *Bmc Cancer* **12**
[147] Ling Y, Wei K, Zou F and Zhong S 2012 *Int. J. Pharm.* **430** 266
[148] Shao H, Yoon T J, Liong M, Weissleder R and Lee H 2010 *Beilstein J Nanotechnol* **1** 142
[149] Fan H M, Olivo M, Shuter B, Yi J B, Bhuvaneswari R, Tan H R, Xing G C, Ng C T, Liu L, Lucky S S, Bay B H and Ding J 2010 *J. Am. Chem. Soc.* **132** 14803
[150] Cheon J and Lee J H 2008 *Accounts Chem. Res.* **41** 1630
[151] Tallury P, Payton K and Santra S 2008 *Nanomedicine* **3** 579
[152] Gu H W, Zheng R K, Zhang X X and Xu B 2004 *J. Am. Chem. Soc.* **126** 5664
[153] Gao J H, Zhang B, Gao Y, Pan Y, Zhang X X and Xu B 2007 *J. Am. Chem. Soc.* **129** 11928
[154] Lim E K, Yang J, Dinney C P N, Suh J S, Huh Y M and Haam S 2010 *Biomaterials* **31** 9310
[155] Selvan S T, Patra P K, Ang C Y and Ying J Y 2007 *Angew. Chem. Int. Ed.* **46** 2448
[156] Yang Y M, Aw J X, Chen K, Liu F, Padmanabhan P, Hou Y L, Cheng Z and Xing B G 2011 *Chem. Asian J.* **6** 1381
[157] Park J H, von Maltzahn G, Ruoslahti E, Bhatia S N and Sailor M J 2008 *Angew. Chem. Int. Ed.* **47** 7284
[158] Gao J H, Zhang W, Huang P B, Zhang B, Zhang X X and Xu B 2008 *J. Am. Chem. Soc.* **130** 3710
[159] Xu C, Xie J, Ho D, Wang C, Kohler N, Walsh E G, Morgan J R, Chin Y E and Sun S 2008 *Angew. Chem. Int. Ed.* **47** 173
[160] Gu H W, Yang Z M, Gao J H, Chang C K and Xu B 2005 *J. Am. Chem. Soc.* **127** 34
[161] Jiang J, Gu H, Shao H, Devlin E, Papaefthymiou G C and Ying J Y 2008 *Adv. Mater.* **20** 4403
[162] Xie J, Zhang F, Aronova M, Zhu L, Lin X, Quan Q, Liu G, Zhang G, Choi K Y, Kim K, Sun X, Lee S, Sun S, Leapman R and Chen X 2011 *ACS Nano* **5** 3043
[163] Reddy G R, Bhojani M S, McConville P, Moody J, Moffat B A, Hall D E, Kim G, Koo Y E L, Woolliscroft M J, Sugai J V, Johnson T D, Philbert M A, Kopelman R, Rehemtulla A and Ross B D 2006 *Clin. Cancer Res.* **12** 6677
[164] Grootendorst D J, Jose J, Fratila R M, Visscher M, Velders A H, Ten Haken B, Van Leeuwen T G, Steenbergen W, Manohar S and Ruers T J M 2013 *Contrast Media Mol. Imaging* **8** 83
[165] O'Grady K 2009 *J. Phys. D: Appl. Phys.* **42** 224001
[166] Berry C C 2009 *J. Phys. D: Appl. Phys.* **42** 224003
[167] Roca A G, Costo R, Rebolledo A F, Veintemillas-Verdaguer S, Tartaj P, Gonzalez-Carreno T, Morales M P and Serna C J 2009 *J. Phys. D: Appl. Phys.* **42** 224002
[168] Wang S X, Zhou Y and Sun W T 2009 *Materials Science & Engineering C-Biomimetic and Supramolecular Systems* **29** 1196
[169] Berry C C and Curtis A S G 2003 *J. Phys. D: Appl. Phys.* **36** R198
[170] Tartaj P, Morales M D, Veintemillas-Verdaguer S, Gonzalez-Carreno T and Serna C J 2003 *J. Phys. D: Appl. Phys.* **36** R182